Spring 2022

Magel2 and Hypothalamic POMC Neuron Modulation of Infant Mice Isolation-Induced Vocalizations

Gabriela M. Bosque Ortiz
Yale University Graduate School of Arts and Sciences, bosque.ortiz.gabriela@gmail.com

Abstract

Magel2 and Hypothalamic POMC Neuron Modulation of Infant Mice Isolation-Induced Vocalizations

Gabriela M. Bosque Ortiz

2022

The proper development of infant mammals depends on infant vocalization. Infants vocalize (i.e., cry) when isolated from their caregivers, attracting their attention to receive nurture. Impaired vocal behavior can lead to maternal neglect and even death in some species. Similar to humans and other mammals, infant mice vocalize upon isolation from their nest and decrease vocalizations when reunited with their mother or littermates. Mouse pups vocalize above the human audible range, emitting ultrasonic vocalizations (USV). My thesis investigated the effects of the imprinted gene, *Magel2*, on mouse vocal behavior (Chapter 2; published in *Genes, Brain, and Behavior*) and also identified a population of neurons in the hypothalamus that modulate vocal behavior (Chapter 3; unpublished).

Magel2 (or *MAGEL2* in humans) is a paternal imprint gene and its loss of function is associated with atypical behaviors seen in autism spectrum disorders and in Prader-Willi Syndrome. In Chapter 2, I report the study of the emission of ultrasonic vocalizations by *Magel2* deficient pups during their early postnatal development. I recorded and analyzed vocalizations from *Magel2* deficient pups and their wildtype littermates during isolation from the home nest at postnatal days 6-12. I describe my findings showing that *Magel2* deficient pups present a lower rate of vocalizations and altered vocal repertoire compared to wildtype littermates. Moreover, these results correlate with altered behavior

of the dam towards their own pups: dams prefer to retrieve their wildtype offspring compared to their *Magel2* deficient offspring. These results suggest that *Magel2* affects the expression of infant vocalizations and also modulates the expression of maternal behaviors.

In Chapter 3, I describe my discovery of a population of neurons in the mammalian hypothalamus that modulate the emission of ultrasonic vocalizations in mouse pups. The brain opioid theory of social attachment postulates that pups release opioids in the brain during caretaking behaviors, which reinforces the attachment bond between pups and caretakers. From the three main receptors known to bind different types of endogenous opioids, μ-opioid receptors (ORPM1) are thought to be important in the modulation of attachment behaviors and, consequently, emission of vocalizations. Whether endogenous opioids act on ORPM1-expressing cells to modulate vocalizations is unknow.

Since the opioid with highest affinity for ORPM1 is β-endorphin, I determined the contribution of neurons that produce β-endorphin—POMC neurons—in infant vocalizations. Using genetic, chemogenomic, and pharmacogenetic approaches, my results show that mice deficient for β-endorphin vocalize more than controls, an effect that is mimicked by a pharmacological blocker of opioid receptors, naloxone. Importantly, naloxone fails to increase vocalizations in β-endorphin deficient pups. Moreover, using chemogenetics, activation of POMC neurons in the hypothalamus suppresses the emission of vocalizations, while ablation of these neurons increased the number of vocalizations. Finally, I show that activation of POMC neurons in mice deficient for the *Orpm1* does not suppress the emission of vocalizations. Together, the results in Chapter 3 suggest that the emission of infant vocalizations is modulated by

POMC neurons in the hypothalamus via the release of beta-endorphin that signals in downstream mu-opioid receptors.

In sum, this dissertation reports novel findings on the effect of the *Magel2* gene and of hypothalamic POMC neurons in the modulation of infant vocalization. As we learn more about the physiological and neuronal responses to distress that occurs in infants, we will more accurately understand the mechanisms involved in the affective emotional states that contribute to the normal and pathological development of infants.

Magel2 and Hypothalamic POMC Neuron Modulation of Infant Mice Isolation-Induced Vocalizations

A Dissertation

Presented to the Faculty of the Graduate School

Of

Yale University

In Candidacy for the Degree of

Doctor of Philosophy

By

Gabriela Maria Bosque Ortiz

Dissertation Director: Marcelo O. Dietrich

May, 2022

Dedication:

I want to give a special thank you and dedicate this thesis to my aunt; Maria del Lourdes Bosque Fernandez. She introduced me to scientific research in the microbiology lab of La Inter de Aguadilla, Puerto Rico. Her love for science was contagious and her impact on me will last forever.

What I admire most about titi Lourdes, is her dedication to lift others up with sense of humor and warmth. Hence, she is a great mentor as seen with her experience as a microbiologist, a teacher, a *catequista*, a *cursillista*, a *legionaria*, and on and on!

Most importantly, Titi Lourdes has taught me to love learning. Besides science, she loves literature and theater. As a toddler, she would teach me how to recite poems that I would then perform to the family. Most of the time; however, rather than poems, I would beg her to teach me jokes since she always has good ones; most of them I still share today.

Thank you, Titi Lourdes, for all your strength, wisdom, and support. T.Q.M.

1. Introduction

1.1 Infant vocalization is an innate behavior conserved among mammals

Altricial mammals, including humans, are born in an immature state. They depend on parental care and nurture for development and survival in the early postnatal period. As a behavior adaption to this dependency, infants vocalize (i.e., cry) when in a situation of distress or discomfort to attract caregiver nurture[1-3] (**Fig 1.1.1A**). Mute or scarce vocalizer mouse pups are neglected by their mothers from an early age and have increased chance of death[4]. In rodents and chicks, mere displacement of infants from their home nest is enough to induce vocal behavior[3,5]. These vocalizations are also referred to as *isolation calls* or *distress calls*. Distress calls are conserved across the vertebrate phylogeny, with many animals sharing similar acquisition, expression, and regulation of this behavior.[2,3,5]

Infant vocalizations are considered innate rather than learned: infants are born with a preprogramed mechanism to vocalize in response to distress. Innate behaviors are genetically encoded and depend on subcortical regions for behavior output[3,6-8] (**Fig 1.1.1B**). Learned behaviors require retaining memories typically through brain regions including the hippocampus, thalamus, amygdala, and cortex[9]. In support of the innate nature of infant vocalizations, infant mice vocalize during the first two weeks of life despite starting to hear—and therefore having an auditory feedback—only after

postnatal day 9 [10]. Moreover, anencephalic human infants, lacking most of the brain except for lower brain motor and limbic regions, emit normal vocalizations. Similar results have been found in rodents, cats and primates [3,8,11-15]. In sum, infant vocalizations are an innate behavior that is conserved across species. This social behavior signals pup social affect and is key in infant-maternal bond. In the next sections, I will introduce how infant vocalizations can be used for experimental research to study the genetic and neurocircuit mechanisms affecting infant behavior.

1.2 Frequency modulation in infant vocalization

The tonal structure of infant vocalizations is shared across many species (**Figure 1.2.1**). (The Lingle lab published an extensive review of infant vocalizations across the animal kingdom and found that infant vocalizations are typically of tonal structure with harmonic components[2].) Rare exceptions include, for example, kangaroos that make broadband noises that sound like cough instead of cry. It is thought that tonal calls are better for distance hearing rather than broadband noises which need to be in close proximity[16].

In most species studied however, vocalization fundamental frequency is the most important feature for maternal response[8,17-19] (**Figure 1.2.1A**). Changes in sound frequency are perceived as "pitch" of the calls representing contours in vocal shape. For example, mule deer and white-tailed deer mothers attend to calls of any infant as long as they vocalized within a species-specific "response range"[19] (**Figure 1.2.1B**). Another example are meerkats which feed young pups as long as the fundamental frequency is within range of the youngest. While older pups may still call, adults will not feed them because of the lower fundamental frequency [20]. Finally, variation in the fundamental

frequency of baby cries is one of the clearest predictors of the distress felt by human adult listeners[21]. In other words, frequency is important for maternal response and the range of the fundamental frequency is widely shared across species.

Mammals also share similar patterns of frequency modulation. Repeated patterns of frequency modulations that give shape to tonal calls across time, have been categorized under different "vocal classes" so similar shaped calls can be grouped together[2,22,23]. The most common vocal class recorded from infant mammals are "chevrons" (a reversed-U, with frequency modulations rising then falling). There are also "flat" and "short" calls (no contours, straight line) and some descending or ascending frequency modulations (incline shape). U shape and compound patterns of modulation are rare classes that were seen across species as well (reverse chevron, frequency steps call types respectively)[2,3]. Figure 3 summarizes vocalization classes and use (**Figure 1.2.2A**).

In mice, by categorizing vocal classes based on their frequency modulation, at least ten different classes of vocalizations occur in infants[1,22,23]. Studies using mice suggest that the emission of vocalizations of different classes is sensitive to maternal rearing of pups as well as pup arousal state. For example, pups from one strain cross-fostered to a mother from a different strain match the vocal class repertoire of mother's strain rather than their own genetic strain[18,24-26]. Another study from our laboratory demonstrated that neurons that promote a negative affective state can specifically modulate the class of vocalizations emitted by mouse pups[27]. In this case, short and flat calls were observed in conditions of low arousal, while calls with frequency and bandwidth changes, such as chevron, were associate with conditions of high arousal or distress[27].

A.

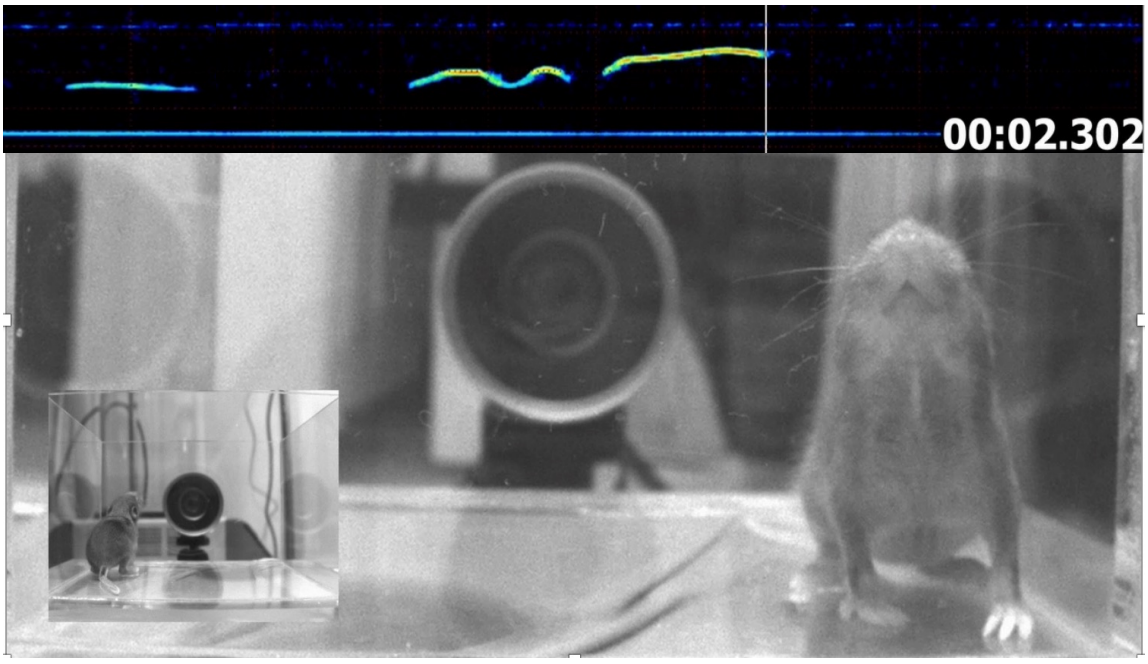
00:02.302

B.

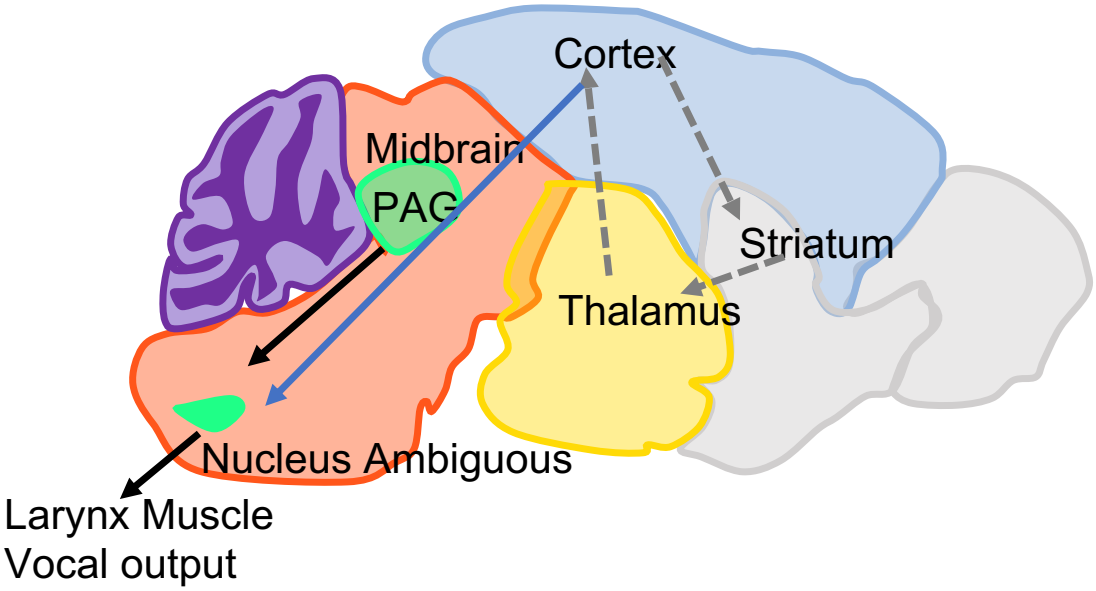
Cortex
Midbrain
PAG
Striatum
Thalamus
Nucleus Ambiguous
Larynx Muscle
Vocal output

Figure 1.1.1. Infant vocalization is an innate behavior. *A) Still image of video recording from isolated mouse pup at 12 days old. Spectrogram of real-time vocalizations seen above (Dietrich lab). B) Brain regions involved in the control of vocal behavior in rodents: non-learning pathway traced with black arrows from the midbrain to the larynx. The pathway involved in vocal learning is traced in blue to highlight the cortical influence over the brainstem (Arriaga, 2012).*

Similar pattern emerges as mouse pups age. As pups become more independent of their mothers, they rely less on maternal support and, as a result, they decrease the emission of isolation-induced vocalizations[4,26,28,29]. As pups get older, they mostly emit flat and short calls while younger ages showed a more variable repertoire of frequency modulation patterns. Together these studies suggest that features of infant vocalizations may serve specific purposes to modulate maternal care behavior.

1.3 Regulation of infant distress calls through endogenous opioids

Vertebrates are able to manage pain and motivation in part through regulation of endogenous opioids. The body synthesizes different types of opioids grouped into three peptide categories: Enkephalins, β-Endorphin, Dynorphins[30,31]. Moreover, these peptides are synthesized from pro-peptide expression in the cell (**Figure 1.3.1B**). Opioids can be released as hormones from the pituitary and adrenal gland. Opioids can also be released as neuromodulators from within the brain [30] (**Figure 1.3.1A**). It is thought that opioid modulation in the brain was adapted to cause an analgesic response during stress, similarly to its effects on pain[7,32,33].

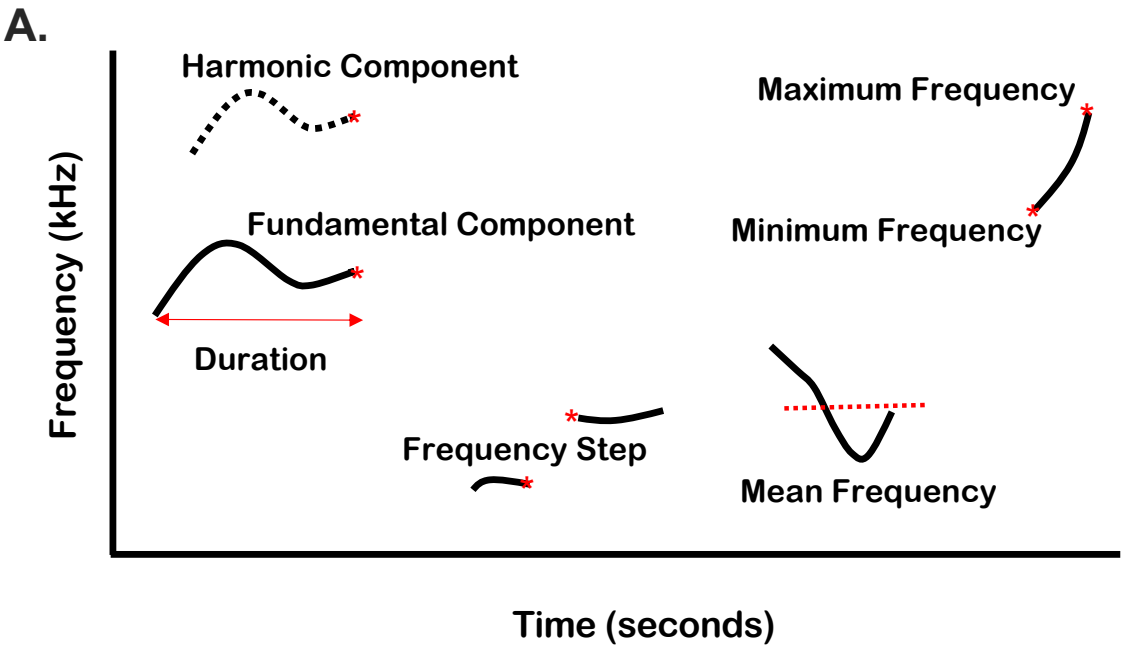
A.
Harmonic Component
Maximum Frequency
Fundamental Component
Minimum Frequency
Duration
Frequency Step
Mean Frequency
Frequency (kHz)
Time (seconds)

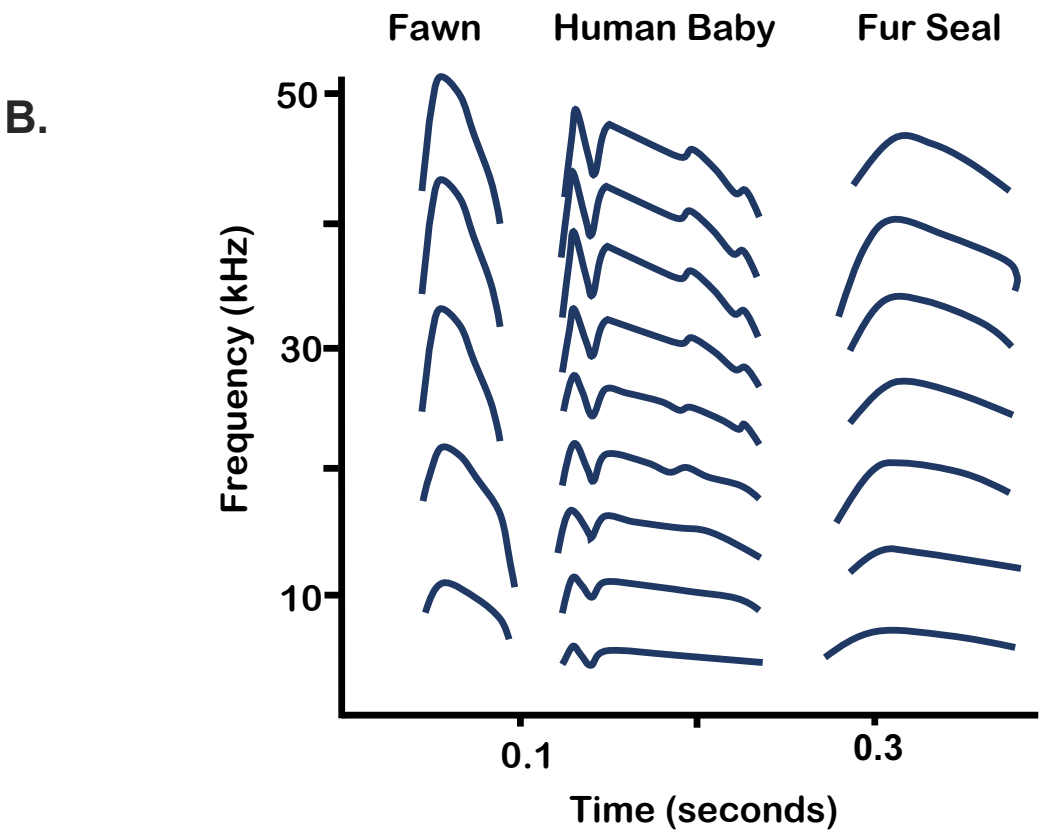
B.
Fawn
Human Baby
Fur Seal
50
30
10
Frequency (kHz)
0.1
0.3
Time (seconds)

Figure 1.2.1. Acoustic structure of infant vocalization. *A) Diagram representing different vocal features that can be measured in vocalizations. B) Tracing of infant vocalization from infant deer (fawn), human infant, and infant fur seal. Vocalizations are of similar frequency range and similar structural shape. Deer mothers react similarly to vocalizations of human and fur seals because of similar spectral features (Lingle, 2012).*

Opioids are mostly known to act as analgesics in response to pain. Hence, endogenous opioids mostly provide an inhibitory tone for neural activity leading to relaxing and sedative effects[31,32,34]. Opioids interact with opioid receptors in order to modulate downstream neural activity. Opioid receptors are grouped in 3 main families: δ (DOR), κ (KOR), and μ (MOR). Different groups of opioids show affinity to at least one of these receptors. For the most part, Dynorphins interact with KOR receptors, Enkephalins with DOR, and Endorphins with MOR[30,35].

Out of the opioid receptors, MOR is thought to strongly modulate social bonding. For example, polymorphisms in MOR gene (Orpm1) influences attachment behavior of infant primates to their mothers. Infant primates with efficient Orpm1 polymorphisms would vocalize more during maternal separation and show maternal social preference[36]. These studies suggest that MOR is important for regulation of social behavior. Moreover, treatment of infants with morphine (a MOR agonist) reduces infant vocalizations while naloxone (a non-specific receptor with high affinity to MOR) increases vocal emission of infant rhesus macaque, rodent, dogs, and chicks during isolation[3,5,7,37,38].

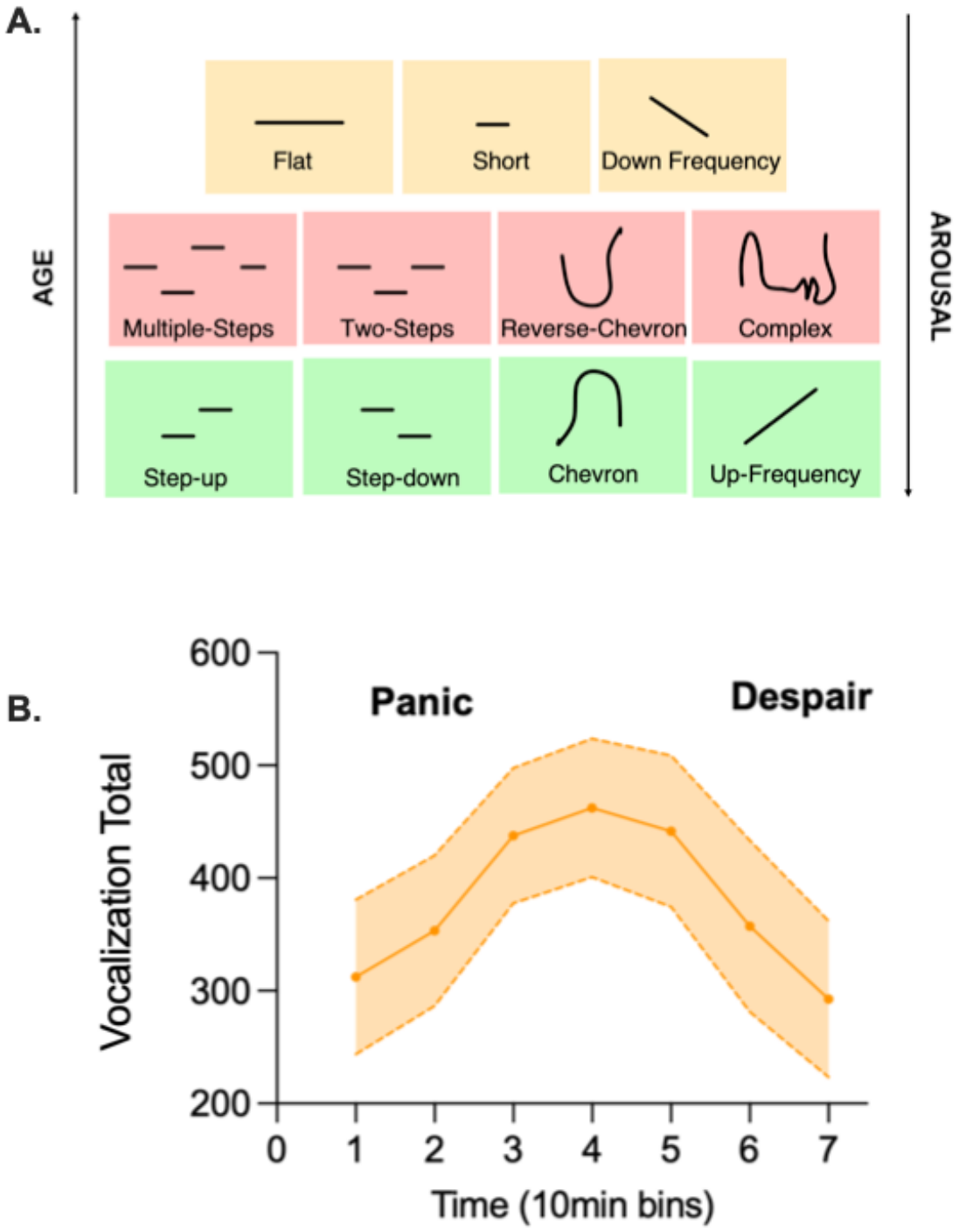

Figure 1.2.2. Infant mouse vocal classes. *A) Visual representation of the different categories of vocal classes based on their morphology on spectrograms. Peak of*

isolation-induced vocalization behavior is seen between P6-P12. During earlier ages (around P6-P8), pups start to use one step, chevrons and frequency modulation calls when distressed. At later ages like P9-P11, pups further expand their repertoire with multiple steps vocalizations; although rare, they can also make reverse chevron and complex vocals. Pups approaching independence (P12-P14) use simple calls with little frequency changes; this includes flat, shorts and down-frequency calls. Mice use of isolation-induced USVs diminishes after first two weeks of life. B) Infant mouse vocalization during 70-minute isolation. B6 mouse were used at P9-P10 (N = 13). Infant vocalization increases rate during first half of isolation period. Panksepp describes this phase as panic and is characterized with high arousal behavior. With prolonged isolation, vocalization rate starts to drop in what Panksepp referred to as the despair phase with low locomotion and depressive-like behaviors.

Based on the evidence that opioids modulate the behaviors of infants, Panksepp proposed the Brain-Opioid Theory of Social Attachment (BOTSA)[39]. In short, the theory suggests that bouts of opioid are released during social interactions, which promotes a positive or rewarding state in pups. For example, when pups are removed from their home nest, opioid signaling diminishes and the pup transitions to a negative affective state. Lower opioid levels motivate pups to reach out of social interaction through vocalization, in order to get back to a positive state. Social reunion promotes opioid release in pups. This social seeking behavior is thought to be modulated through MOR[2,3,39]. However, if mom does not respond to pup vocalizations, pups transfer to a state of despair. During prolonged isolations, pup vocal rate starts to drop, and they move less[32,40] (**Figure 1.3.1B**). Even though endogenous opioids are associated to rewarding affective states and social reunion, Panksepp proposes that despair is also modulated through endogenous opioids, maintaining negative affect[40].

A.

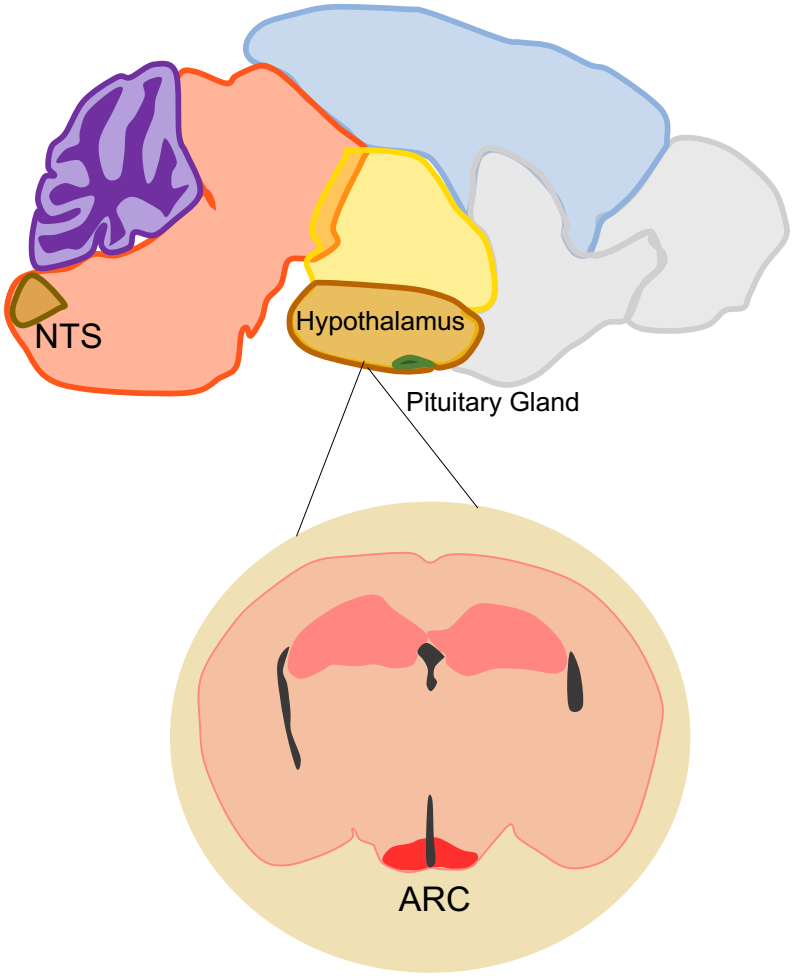
NTS
Hypothalamus
Pituitary Gland
ARC

B.

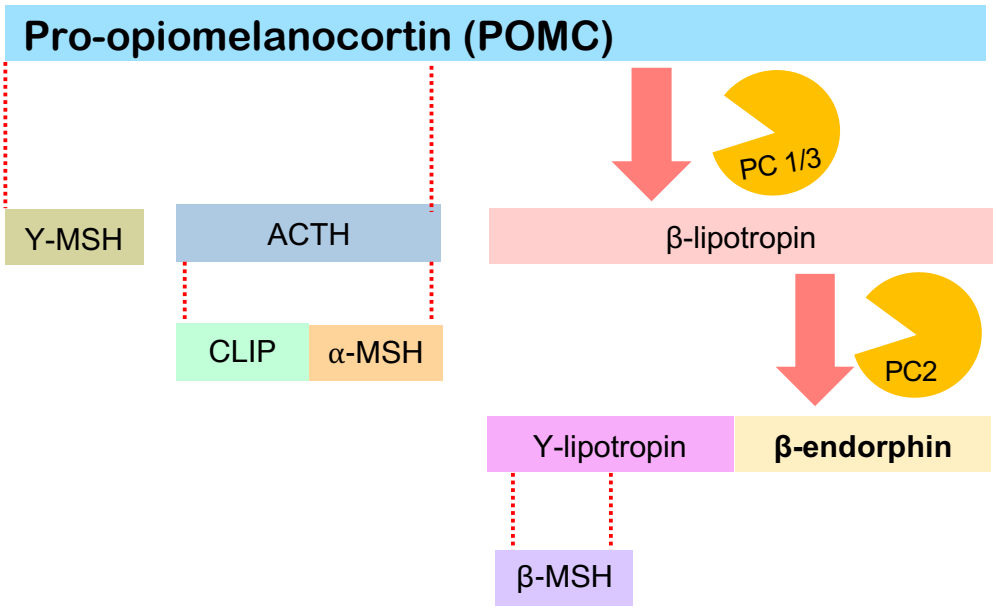
Pro-opiomelanocortin (POMC)
PC 1/3
Y-MSH
ACTH
β-lipotropin
CLIP
α-MSH
PC2
Y-lipotropin
β-endorphin
β-MSH

Figure 1.3.1. Hypothalamic modulation of infant vocal behavior. *Infant mouse vocalization during 70-minute isolation. B6 mouse were used at P9-P10 (N = 13). Infant vocalization increases rate during first half of isolation period. Panksepp describes this phase as panic and is characterized with high arousal behavior. With prolonged isolation, vocalization rate starts to drop in what Panksepp referred to as the despair phase with low locomotion and depressive-like behaviors.*

Little is known about the regulation of despair in pups. However, recent studies in adult rodents suggest that endogenous opioids that bind to MOR can regulate despair through "stress-induced analgesia" (SIA). SIA is evoked through the brain in mild and acute stress as a way to cope with ongoing negative state[41]. For example, when mice are dropped in a tub of water, they actively try to jump out. If they are unable to quickly escape, mice transition to longer periods of time floating than trying to escape. However, mice that are not able to synthesize β-Endorphin—the endogenous opioid with the highest affinity for MOR—do not make this last transition and continually try to escape for longer periods of time[42]. In another study, β-Endorphin deficient mice were more likely to be aggressive with aggressive conspecifics in comparison to control. In other words, β-Endorphin promotes despair behavior in face of an aggressor to cope with social stress[43].

1.4 Hypothalamus role in genetic and neural regulation of infant vocalizations

Within the CNS, the hypothalamus senses homeostatic processes and respond when optimal physiological state is unbalanced. Part of hypothalamic response includes behavior manipulation. For example, within the hypothalamus arcuate nucleus (ARC),

there are two neural groups that produce either Agouti-related peptide (Agrp) or Proopiomelanocortin (POMC). These neurons are heavily involved in keeping nutritional homeostasis in adult mice. Under starved conditions Agrp neurons promote food-foraging behavior (exploration); once food cues are detected, POMC neurons signal for food consummation and satisfaction (exploitation)[44,45].

The hypothalamus is also associated with the regulation of developmental milestones through imprint genes. Imprint genes are a parent-of-origin epigenetic mechanism that controls genetic expression[46]. Here, normal organism development depends on a delicate balance in which paternal gene expression is focused on energy intake; and maternal gene expression stunts growth and energy expenditure.

In summary, the hypothalamus is an important brain region for regulation of infant pup distressed vocal behavior (**Figure 1.3.1**). The next two chapters will bring new insights into the genetic and neural mechanisms regulating infant vocalization in mouse pups within the hypothalamus. First, I will describe results using genetic manipulation to study the effects of epigenetic mechanisms on the ontogeny of infant vocalization. Second, I will provide evidence for the modulation of isolation-induced vocalizations and despair in mouse pups by an opioid signaling originated from the hypothalamus. Ultimately, this body of work sheds light into the rise and adaptation of mammalian vocal behavior as well as the requisites for a healthy neural development.

1.5 References

1. D'Amato FR, Scalera E, Sarli C, Moles A. Pups call, mothers rush: does maternal responsiveness affect the amount of ultrasonic vocalizations in mouse pups? *Behav Genet.* 2005;35(1):103-112.
2. Lingle S, Wyman MT, Kotrba R, Teichroeb LJ, Romanow CA. What makes a cry a cry? A review of infant distress vocalizations. *Current Zoology.* 2012;58(5):698-726.
3. Newman JD. Neural circuits underlying crying and cry responding in mammals. *Behav Brain Res.* 2007;182(2):155-165.
4. Bosque Ortiz GM, Santana GM, Dietrich MO. Deficiency of the paternally inherited gene Magel2 alters the development of separation-induced vocalization and maternal behavior in mice. *Genes Brain Behav.* 2022;21(1):e12776.
5. Panksepp J, Meeker R, Bean NJ. The neurochemical control of crying. *Pharmacol Biochem Behav.* 1980;12(3):437-443.
6. Scheller RH, Jackson JF, McAllister LB, Rothman BS, Mayeri E, Axel R. A single gene encodes multiple neuropeptides mediating a stereotyped behavior. *Cell.* 1983;32(1):7-22.
7. Panksepp J, Herman BH, Vilberg T, Bishop P, DeEskinazi FG. Endogenous opioids and social behavior. *Neurosci Biobehav Rev.* 1980;4(4):473-487.
8. Arriaga G, Zhou EP, Jarvis ED. Of mice, birds, and men: the mouse ultrasonic song system has some features similar to humans and song-learning birds. *PLoS One.* 2012;7(10):e46610.
9. Wei D, Talwar V, Lin D. Neural circuits of social behaviors: Innate yet flexible. *Neuron.* 2021;109(10):1600-1620.

10. Hammerschmidt K, Reisinger E, Westekemper K, Ehrenreich L, Strenzke N, Fischer J. Mice do not require auditory input for the normal development of their ultrasonic vocalizations. *BMC Neurosci.* 2012;13:40.

11. Barnet A, Bazelon M, Zappella M. Visual and auditory function in an hydranencephalic infant. *Brain Res.* 1966;2(4):351-360.

12. Kyuhou S, Gemba H. Two vocalization-related subregions in the midbrain periaqueductal gray of the guinea pig. *Neuroreport.* 1998;9(7):1607-1610.

13. Middlemis-Brown JE, Johnson ED, Blumberg MS. Separable brainstem and forebrain contributions to ultrasonic vocalizations in infant rats. *Behav Neurosci.* 2005;119(4):1111-1117.

14. Magoun HW, Atlas D, Ingersoll EH, Ranson SW. Associated Facial, Vocal and Respiratory Components of Emotional Expression: An Experimental Study. *J Neurol Psychopathol.* 1937;17(67):241-255.

15. Jurgens U, Ploog D. Cerebral representation of vocalization in the squirrel monkey. *Exp Brain Res.* 1970;10(5):532-554.

16. Carter GG, Logsdon R, Arnold BD, Menchaca A, Medellin RA. Adult vampire bats produce contact calls when isolated: acoustic variation by species, population, colony, and individual. *PLoS One.* 2012;7(6):e38791.

17. Yurlova DD, Volodin IA, Ilchenko OG, Volodina EV. Rapid development of mature vocal patterns of ultrasonic calls in a fast-growing rodent, the yellow steppe lemming (Eolagurus luteus). *PLoS One.* 2020;15(2):e0228892.

18. Ashbrook DG, Roy S, Clifford BG, et al. Born to Cry: A Genetic Dissection of Infant Vocalization. *Front Behav Neurosci.* 2018;12:250.

19. Lingle S, Riede T. Deer mothers are sensitive to infant distress vocalizations of diverse mammalian species. *Am Nat.* 2014;184(4):510-522.

20. Madden JR, Kunc HJP, English S, Clutton-Brock TH. Why do meerkat pups stop begging? *Animal Behaviour.* 2009;78(1):85-89.

21. LaGasse LL, Neal AR, Lester BM. Assessment of infant cry: acoustic cry analysis and parental perception. *Ment Retard Dev Disabil Res Rev.* 2005;11(1):83-93.

22. Grimsley JM, Monaghan JJ, Wenstrup JJ. Development of social vocalizations in mice. *PloS one.* 2011;6(3):e17460.

23. Scattoni ML, Gandhy SU, Ricceri L, Crawley JN. Unusual repertoire of vocalizations in the BTBR T+tf/J mouse model of autism. *PLoS One.* 2008;3(8):e3067.

24. Wohr M, Dahlhoff M, Wolf E, Holsboer F, Schwarting RK, Wotjak CT. Effects of genetic background, gender, and early environmental factors on isolation-induced ultrasonic calling in mouse pups: an embryo-transfer study. *Behav Genet.* 2008;38(6):579-595.

25. Premoli M, Memo M, Bonini SA. Ultrasonic vocalizations in mice: relevance for ethologic and neurodevelopmental disorders studies. *Neural Regen Res.* 2021;16(6):1158-1167.

26. Heckman J, McGuinness B, Celikel T, Englitz B. Determinants of the mouse ultrasonic vocal structure and repertoire. *Neurosci Biobehav Rev.* 2016;65:313-325.

27. Zimmer MR, Fonseca AHO, Iyilikci O, Pra RD, Dietrich MO. Functional Ontogeny of Hypothalamic Agrp Neurons in Neonatal Mouse Behaviors. *Cell.* 2019;178(1):44-59 e47.

28. Peleh T, Eltokhi A, Pitzer C. Longitudinal analysis of ultrasonic vocalizations in mice from infancy to adolescence: Insights into the vocal repertoire of three wild-type strains in two different social contexts. *PLoS One.* 2019;14(7):e0220238.

29. Elwood RW, Keeling F. Temporal organization of ultrasonic vocalizations in infant mice. *Developmental psychobiology.* 1982;15(3):221-227.

30. Froehlich JC. Opioid peptides. *Alcohol Health Res World.* 1997;21(2):132-136.

31. Corder G, Castro DC, Bruchas MR, Scherrer G. Endogenous and Exogenous Opioids in Pain. *Annu Rev Neurosci.* 2018;41:453-473.

32. Spiaggia A, Bodnar RJ, Kelly DD, Glusman M. Opiate and non-opiate mechanisms of stress-induced analgesia: cross-tolerance between stressors. *Pharmacol Biochem Behav.* 1979;10(5):761-765.

33. Panksepp J, Herman B, Conner R, Bishop P, Scott JP. The biology of social attachments: opiates alleviate separation distress. *Biol Psychiatry.* 1978;13(5):607-618.

34. Watkins LR, Mayer DJ. Organization of endogenous opiate and nonopiate pain control systems. *Science.* 1982;216(4551):1185-1192.

35. Kieffer BL, Gaveriaux-Ruff C. Exploring the opioid system by gene knockout. *Prog Neurobiol.* 2002;66(5):285-306.

36. Barr CS, Schwandt ML, Lindell SG, et al. Variation at the mu-opioid receptor gene (OPRM1) influences attachment behavior in infant primates. *Proc Natl Acad Sci U S A.* 2008;105(13):5277-5281.

37. Kalin NH, Shelton SE, Barksdale CM. Opiate modulation of separation-induced distress in non-human primates. *Brain Res.* 1988;440(2):285-292.

38. Herman BH, Panksepp J. Ascending endorphin inhibition of distress vocalization. *Science.* 1981;211(4486):1060-1062.

39. Nelson EE, Panksepp J. Brain substrates of infant-mother attachment: contributions of opioids, oxytocin, and norepinephrine. *Neurosci Biobehav Rev.* 1998;22(3):437-452.

40. Panksepp J, Watt D. Why does depression hurt? Ancestral primary-process separation-distress (PANIC/GRIEF) and diminished brain reward (SEEKING) processes in the genesis of depressive affect. *Psychiatry.* 2011;74(1):5-13.

41. Amit Z, Galina ZH. Stress-induced analgesia: adaptive pain suppression. *Physiol Rev.* 1986;66(4):1091-1120.

42. Rubinstein M, Mogil JS, Japon M, Chan EC, Allen RG, Low MJ. Absence of opioid stress-induced analgesia in mice lacking beta-endorphin by site-directed mutagenesis. *Proc Natl Acad Sci U S A.* 1996;93(9):3995-4000.

43. Vaanholt LM, Turek FW, Meerlo P. Beta-endorphin modulates the acute response to a social conflict in male mice but does not play a role in stress-induced changes in sleep. *Brain Res.* 2003;978(1-2):169-176.

44. Quarta C, Claret M, Zeltser LM, et al. POMC neuronal heterogeneity in energy balance and beyond: an integrated view. *Nat Metab.* 2021;3(3):299-308.

45. Cisek P. Resynthesizing behavior through phylogenetic refinement. *Atten Percept Psychophys.* 2019;81(7):2265-2287.

46. Perez JD, Rubinstein ND, Dulac C. New Perspectives on Genomic Imprinting, an Essential and Multifaceted Mode of Epigenetic Control in the Developing and Adult Brain. *Annu Rev Neurosci.* 2016;39:347-384.

Chapter 2: Paternal-inherited gene, Magel2, alters the development of mice separation-induced vocalization and maternal behavior

2.1 Abstract

The behavior of offspring results from the combined expression of maternal and paternal genes. Genomic imprinting silences some genes in a parent-of-origin specific manner, a process that, among all animals, occurs only in mammals. How genomic imprinting affects the behavior of mammalian offspring, however, remains poorly understood. Here, we studied how the loss of the paternally inherited gene *Magel2* in mouse pups affects the emission of separation-induced ultrasonic vocalizations (USV). Using quantitative analysis of more than one hundred thousand USVs, we characterized the rate of vocalizations as well as their spectral features from postnatal days 6 to 12 (P6-P12), a critical phase of mouse development that covers the peak of vocal behavior in pups. Our analyses show that *Magel2* deficient offspring emit separation-induced vocalizations at lower rates and with altered spectral features mainly at P8. We also show that dams display altered behavior towards their own *Magel2* deficient offspring at this age. In a test to compare the retrieval of two pups, dams retrieve wildtype control pups first and faster than *Magel2* deficient offspring. These results suggest that the loss of *Magel2* impairs the expression of separation-induced vocalization in pups as well as maternal behavior at a specific age of postnatal development, both of which support the pups' growth and development.

2.2 Introduction

For the normal development, mammalian offspring need copies from both maternal and paternal genomes. Some genes, however, are expressed in a parent-of-origin specific manner. In other words, some genes are always expressed when inherited from the mother and some genes are always expressed when inherited from the father[1-3]. The process that regulates the expression of genes in a parent-of-origin specific manner is called genomic imprinting[4].

Genomic imprinting depends on epigenetic modifications of the genome. These modifications do not alter the sequence of the DNA but the chemical structure of the DNA, thereby leading to altered gene expression[1,4]. For example, an imprinted gene can be silenced in the maternal genome, and only the paternal allele will be expressed in the offspring (or vice-versa). Thus far, genomic imprinting has only been found in flowering plants and mammals[1,2]

The adaptive value of genomic imprinting remains a matter of intense theorization. A prevailing theory on the effects of genomic imprinting, known as the kinship theory[5-7], posits that maternal genes balance the energy investment of the mother between offspring survival and her own while paternal genes favor offspring survival alone. For example, the expression of paternal genes in the offspring would favor growth, while the expression of maternal genes would stunt growth[2,8-10]. The influence of imprinted genes is not restricted to growth, however. Imprinted genes are also primarily involved in brain development and in social behaviors[2,9,11-13].

Consider, for example, a series of imprinted genes in human chromosome 15 that are paternally inherited[14,15]. The deletion of these paternally inherited genes in chromosome 15 leads to neurodevelopmental disorders, such as Prader-Willi syndrome (PWS). PWS presents with hypotonia and poor feeding early in life, followed by hyperphagia, alteration in social behavior, and cognitive deficits[16,17]. It should be noted that because PWS involves several genes in human chromosome 15, it masks the relative contribution of single imprinted genes on the phenotype of the offspring. Among the PWS-related genes, MAGEL2 is a candidate gene for some of the clinical features of PWS. Humans with loss-of-function mutations in MAGEL2 present clinical aspects of PWS and autism spectrum disorders[18,19], suggesting that this single paternally inherited gene supports at least some of the developmental alterations found in PWS. In agreement with the clinical features of MAGEL2 deficiency in humans, *Magel2* deficient mice show impairments in growth and adult social behaviors[10,20]. Despite these previous studies, a more systematic investigation of the effects of imprinted genes on behavior is necessary to understand the adaptive value of these genetic modifications in mammals.

We reasoned that investigating the effects of imprinted genes on offspring behavior during the early postnatal period—when the exchange of resources between the mother and the offspring is most important—can help shed light on the adaptive value of genomic imprinting. Towards this end, we studied how the loss of paternally inherited *Magel2* affects the vocal behavior of mouse pups when separated from their dams[21-24], as separation-induced vocalizations signal the needs of the pups to the dams[25-27]. In contrast to human babies, mouse pups vocalize in the ultrasonic frequency range (30 - 120 kHz)[21,22,28], which humans cannot hear. In order to survey the vocal behavior of mice, we recorded the emission of ultrasonic vocalizations (USVs) when pups were separated from the home nest. We performed these studies at postnatal days 6, 8, 10,

and 12, since it is during this phase of mouse development that the peak expression of separation-induced vocalizations typically occurs[22,23,29]. We then used VocalMat[30] to perform quantitative analysis of mouse vocal behavior. Moreover, we employed a maternal retrieval assay to test the effects of the loss of paternally inherited *Magel2* on maternal behavior towards the offspring[31]. Our analysis shows that in mouse pups the deficiency of *Magel2* impairs the expression of separation-induced vocalizations. This deficiency also reduces maternal retrieval behavior towards *Magel2* deficient pups compared to non-deficient siblings.

2.3 Results

2.3.1 Early waning of vocal behavior in *Magel2*$^{m+/p-}$ deficient pups

To investigate the effects of paternally inherited *Magel2* on the vocal behavior of infant mice, we crossed heterozygote males for *Magel2* deficiency with wildtype females. From this cross, we generated *Magel2* deficient offspring (*Magel2*$^{m+/p-}$) that carry the null allele from the father (p−) and the imprinted allele from the mother (m+). This cross also generates wildtype littermates (*Magel2*$^{m+/p+}$), used as experimental controls. As previously reported[8,10], *Magel2*$^{m+/p-}$ pups display lower body mass compared to controls (genotype: $F_{1, 181} = 19.71$, $P < 10^{-4}$; age: $F_{3, 181} = 69.64$, $P < 10^{-10}$; genotype x age: $F_{3, 181} = 0.02$, $P = 0.99$; two-way ANOVA; **Figure 2.7.1**). Post-hoc analysis shows a significant difference in body mass between genotypes only at P12 (control: 6.08 ± 0.14 g; *Magel2*$^{m+/p-}$: 5.51 ± 0.20 g; $P = 0.04$; Holm-Šídák test; **Figure 2.7.1**).

We recorded the emission of USVs during 20 minutes of separation from the home nest at different postnatal ages (P6, P8, P10, and P12; **Figure 2.3.1A**). First, we analyzed the total number of USVs emitted during the period of separation using two-way ANOVA.

We found a significant effect of genotype, age, and interaction between genotype and age (genotype: $F_{1, 181} = 20.61$, $P < 10^{-4}$; age: $F_{3, 181} = 11.80$, $P < 10^{-6}$; genotype x age: $F_{3, 181} = 3.90$, $P = 0.01$; **Figure 2.3.1B**). Post-hoc analysis (Holm-Šídák test) shows that the total number of USVs is similar among groups at P6 (control: 991 ± 139 USVs; *Magel2*$^{m+/p-}$: 787 ± 130 USVs; $P = 0.75$), P10 (control: 503 ± 45 USVs; *Magel2*$^{m+/p-}$: 466 ± 70 USVs; $P = 0.98$), and P12 (control: 594 ± 71 USVs; *Magel2*$^{m+/p-}$: 345 ± 46 USVs; $P = 0.06$) (**Figure 2.3.1B**). Compared to controls, however, *Magel2*$^{m+/p-}$ pups show a ≈53% reduction in the emission of USVs at P8 (control: 1045 ± 100 USVs; *Magel2*$^{m+/p-}$: 495 ± 65 USVs; $P < 10^{-4}$). We also analyzed the data in 5-minute intervals and found similar effects of *Magel2* deficiency on the rate of vocalizations (**Figure 2.7.2**). Moreover, separating our analysis in females and males show similar effects of genotype and age (**Figure 2.3.1C-D** and **Table S1**). (Because we did not find differences in the rate of vocalization, we have pooled males and females in all further analysis). In sum, our results thus far show age-specific reductions in the emission of USVs in *Magel2*$^{m+/p-}$ mice, suggesting a non-sex specific effect for paternally inherited *Magel2* on the vocal behavior of the offspring.

The emission of USVs occurs when the breathing musculature contracts, expelling air from the lungs and propelling it through the larynx[32,33]. Since previous reports found that *Magel2*$^{m+/p-}$ mice display hypotonia[32], we put forward the hypothesis that the low rate of USV emission in *Magel2* deficient pups is due to a lower capacity to expel air from the lungs. To rule out this hypothesis, we measured the intensity (or volume, in decibels) of the USVs. Since the intensity of the USVs relates to the pressure by which the air is expelled through the larynx[33], a lower intensity is expected in cases of hypotonia. This analysis shows that the intensity of the emitted USVs between *Magel2*$^{m+/p-}$ mice and controls is similar in all ages tested (genotype: $F_{1, 181} = 2.67$, $P = 0.10$; age: $F_{3, 181} = 2.33$,

P = 0.08; genotype x age: $F_{3, 181}$ = 0.78, P = 0.51; two-way ANOVA; **Figure 2.3.1E**). Thus, hypotonia does not seem to be a factor of primary significance for the lower rate of USV emission in *Magel2*$^{m+/p-}$ mice.

Drops in body temperature in immature mouse pups can influence the emission of USVs[34,35]. For example, previous reports show that drops in body temperature during separation inversely correlates with the rate of emission of USVs in mice[34,35]. Based on these observations, in a cohort of pups, we tested their body surface temperature at the end of the 20-minute separation period using thermal imaging. This analysis shows that the body temperature of *Magel2*$^{m+/p-}$ mice and controls is similar in all ages tested (genotype: $F_{1, 26}$ = 0.19, P < 0,67; age: $F_{2, 37}$ = 80.70, $P < 10^{-10}$; genotype x age: $F_{2,38}$= 0.02, P = 0.30; two-way ANOVA; **Figure 2.3.1F).** Thus, we concluded that an altered capacity to maintain body temperature is not a causal (or confounding) factor that explains the differences in the emission of USVs between *Magel2*$^{m+/p-}$ and control pups.

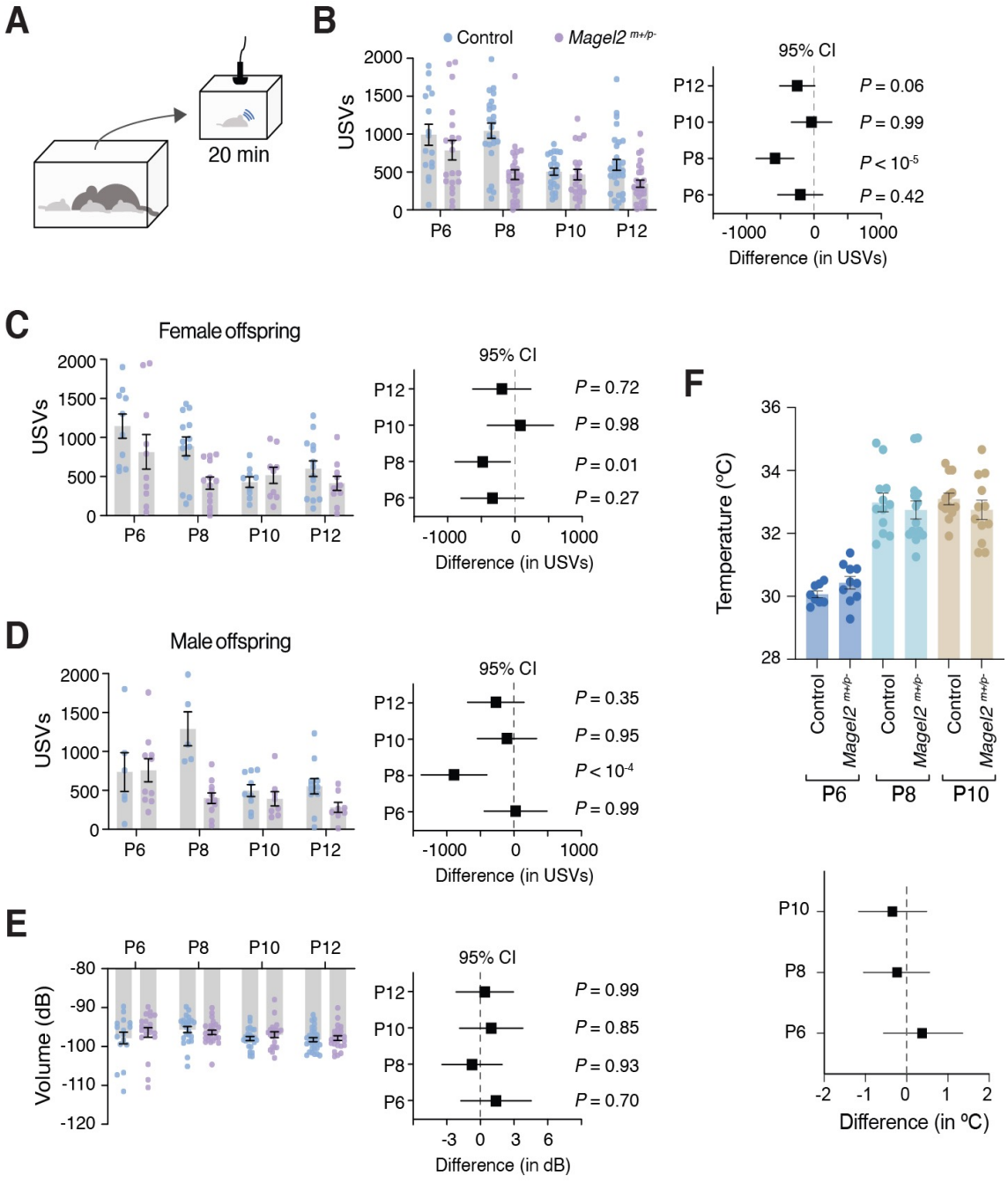
A
20 min
B
Control
Magel2 m+/p-
USVs
2000
1500
1000
500
0
P6
P8
P10
P12
95% CI
P12
P10
P8
P6
P = 0.06
P = 0.99
P < 10-5
P = 0.42
-1000
0
1000
Difference (in USVs)
C
Female offspring
USVs
2000
1500
1000
500
0
P6
P8
P10
P12
95% CI
P12
P10
P8
P6
P = 0.72
P = 0.98
P = 0.01
P = 0.27
-1000
0
1000
Difference (in USVs)
D
Male offspring
USVs
2000
1500
1000
500
0
P6
P8
P10
P12
95% CI
P12
P10
P8
P6
P = 0.35
P = 0.95
P < 10-4
P = 0.99
-1000
0
1000
Difference (in USVs)
E
P6
P8
P10
P12
Volume (dB)
-80
-90
-100
-110
-120
95% CI
P12
P10
P8
P6
P = 0.99
P = 0.85
P = 0.93
P = 0.70
-3
0
3
6
Difference (in dB)
F
Temperature (°C)
36
34
32
30
28
Control
Magel2 m+/p-
Control
Magel2 m+/p-
Control
Magel2 m+/p-
P6
P8
P10
P10
P8
P6
-2
-1
0
1
2
Difference (in °C)

Figure 2.3.1 Magel2 deficiency affects USV emission at P8 *(**A**) Schematic of the protocol used to record separation-induced USVs in mice (from P6 to P12); pups are separated from the home nest in a new chamber equipped with an ultrasonic microphone and recorded for 20 minutes. (**B**) Total number of USVs emitted by control (blue) and Magel2 deficient (purple) littermates at P6, P8, P10, and P12; right panel denotes the 95% confidence intervals as a measure of effect size. (**C**) Similar to (B), but only considering female pups. (**D**) Similar to (B), but only considering male pups. (**E**) Average intensity of the USVs measured in decibels; right panel denotes the 95% confidence intervals as a measure of effect size. The sample sizes for control and Magel2 deficient pups are: P6, n = 16 and 20; P8, n = 23 and 28; P10, n = 23 and 20; and P12, n = 30 and 28, respectively. (**F**) Bar chart of body surface temperature at each age tested. Lower panel denotes the 95% confidence intervals as a measure of effect size. No statistical differences between groups were found (note that all confidence intervals cross zero). In (F), the sample sizes for control and Magel2 deficient pups are: P6, n = 8 and 10; P8, n = 12 and 15; and P10, n = 13 and 12; respectively. Bars represent mean value with error bars representing SEM and round symbols representing individual values. When plotting the effect sizes, squared symbols and black lines represent 95% confidence intervals calculated as the different between Magel2 deficient and control pups. P values are provided in the figures as calculated using Sidak's multiple comparison test.*

2.3.2 Magel2$^{m+/p-}$ mice emit vocalizations with distinct spectral features

In addition to the rate of separation-induced vocalizations, the spectral features of the USVs also correlate with altered maternal care[36-38]. To test the extent to which *Magel2* deficiency affects the spectral features of USVs across ages, we used two-way ANOVA to analyze the frequency characteristics (pitch) and duration (**Figure 2.3.2A**) of

USVs[30]. We found significant effects of genotype and age for maximal frequency (genotype: $F_{1, 181} = 20.51$, $P < 10^{-4}$; age: $F_{3, 181} = 3.23$, $P = 0.02$; genotype x age: $F_{3, 181} = 6.18$, $P < 10^{-3}$; **Figure 2.3.2B**), bandwidth (genotype: $F_{1, 181} = 9.91$, $P < 10^{-2}$; age: $F_{3, 181} = 6.97$, $P < 10^{-3}$; genotype x age: $F_{3, 181} = 5.92$, $P < 10^{-3}$; **Figure 2.3.2E**), and duration (genotype: $F_{1, 181} = 4.08$, $P = 0.04$; age: $F_{3, 181} = 6.35$, $P < 10^{-3}$; genotype x age: $F_{3, 181} = 2.05$, $P = 0.11$; **Figure 2.3.2F**). In addition, we found a significant effect of genotype for mean frequency (genotype: $F_{1, 181} = 4.86$, $P = 0.02$; age: $F_{3, 181} = 0.24$, $P = 0.87$; genotype x age: $F_{3, 181} = 0.41$, $P = 0.74$; **Figure 2.3.2D**), but not for minimal frequency (genotype: $F_{1, 181} = 0.47$, $P = 0.47$; age: $F_{3, 181} = 1.96$, $P = 0.12$; genotype x age: $F_{3, 181} = 0.48$, $P = 0.69$; **Figure 2.3.2C**). We then used post-hoc analysis (Holm-Šídák test) and found that at P8—but not at P6, P10, or P12—*Magel2*$^{m+/p-}$ mice show significant differences compared to control mice in maximal frequency, bandwidth, and duration (see panels plotting the 95% confidence intervals in **Figure 2.3.2**).

In addition to the main frequency component, USVs can contain harmonics (**Figure 2.3.2G**). We calculated the percentage of USVs with harmonics and found a significantly lower number in *Magel2*$^{m+/p-}$ mice compared to controls at P8 (control: 9.0 ± 1.7 %; *Magel2*$^{m+/p-}$: 3.5 ± 0.8 %; $U = 145$, $P_{2\text{-tailed}} = 0.002$, Mann-Whitney test; **Figure 2.3.2H**) but not at P6 (control: 4.7 ± 0.9 %; *Magel2*$^{m+/p-}$: 3.8 ± 0.6 %; $U = 142.5$, $P_{2\text{-tailed}} = 0.93$, Mann-Whitney test; **Figure 2.3.2H**), P10 (control: 5.8 ± 0.9 %; *Magel2*$^{m+/p-}$: 6.1 ± 1.2 %; $U = 240$, $P_{2\text{-tailed}} = 0.98$, Mann-Whitney test; **Figure 2.3.2H**), or P12 (control: 3.6 ± 0.7 %; *Magel2*$^{m+/p-}$: 5.0 ± 1.5 %; $U = 408.5$, $P_{2\text{-tailed}} = 0.98$, Mann-Whitney test; **Figure 2.3.2H**). In sum, these results suggest that the loss of paternally inherited *Magel2* in mice causes discrete changes in the features of separation-induced vocalizations that are most evident at postnatal day eight.

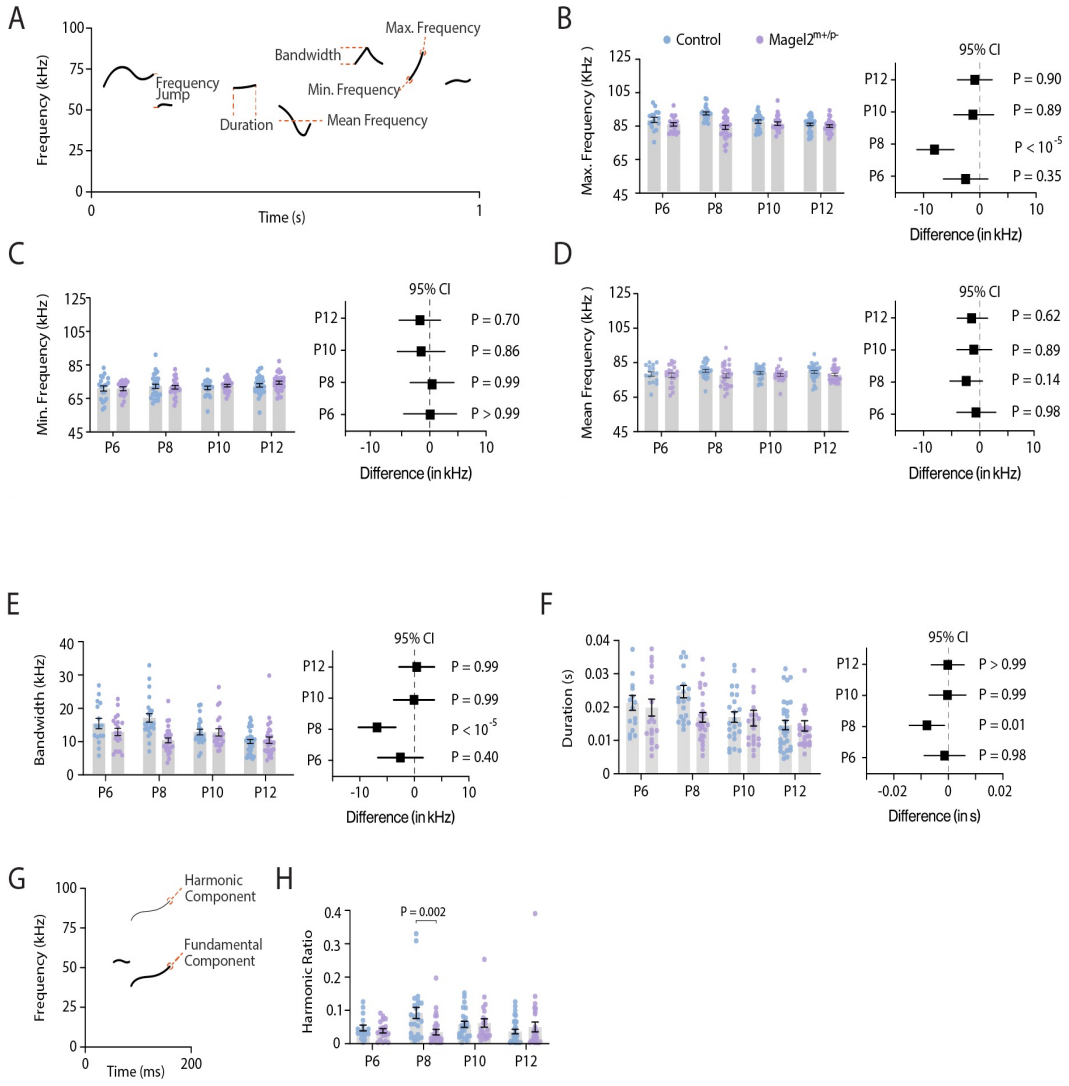
A
Frequency (kHz)
Time (s)
Max. Frequency
Bandwidth
Frequency Jump
Min. Frequency
Duration
Mean Frequency
B
Control
MageI2m+/p-
Max. Frequency (kHz)
95% CI
P12
P10
P8
P6
P = 0.90
P = 0.89
P < 10-5
P = 0.35
Difference (in kHz)
C
Min. Frequency (kHz)
P = 0.70
P = 0.86
P = 0.99
P > 0.99
D
Mean Frequency (kHz)
P = 0.62
P = 0.89
P = 0.14
P = 0.98
E
Bandwidth (kHz)
P = 0.99
P = 0.99
P < 10-5
P = 0.40
F
Duration (s)
P > 0.99
P = 0.99
P = 0.01
P = 0.98
Difference (in s)
G
Harmonic Component
Fundamental Component
Time (ms)
H
Harmonic Ratio
P = 0.002

Figure 2.3.2 Magel2 deficiency affects USV spectral features. *(**A**) Illustration of a spectrogram with the spectro-temporal features measured for each USV. (**B**) Maximum frequency of the USVs emitted by control and Magel2 deficient littermates at P6, P8, P10, and P12; right panel denotes the 95% confidence intervals as a measure of effect size. (**C**) Similar to (B) but plotting the minimum frequency of the USVs. (**D**) Similar to (B) but plotting the mean frequency of the USVs. (**E**) Similar to (B) but plotting the bandwidth of the USVs. (**F**) Similar to (B) but plotting the duration of the USVs. (**G**) Illustration of the spectrogram of a single USV with a harmonic component. (**H**) Ratio of harmonic across all USVs emitted by control and Magel2 deficient littermates. Bars represent mean value with error bars representing SEM and round symbols representing individual values. When plotting the effect sizes, squared symbols and black lines represent 95% confidence intervals calculated as the different between Magel2 deficient and control pups. In B-F, P values are provided in the figures as calculated using Sidak's multiple comparison test post hoc analysis from two-way ANOVA test. In H, P values are provided as calculated using Mann-Whitney test. The sample sizes for control and Magel2 deficient pups are: P6, n = 16 and 20; P8, n = 23 and 28; P10, n = 23 and 20; and P12, n = 30 and 28, respectively.*

2.3.3 Discrete changes in the use of syllable types by *Magel2*$^{m+/p-}$ mice

Mouse pups emit USVs of distinct classes—i.e., syllable types. Thus, the emission of different syllable types could explain the discrete changes in the spectro-temporal features of USVs in *Magel2*$^{m+/p-}$ [28,30,39]. We used a validated software to automatically categorize each USV into one of eleven syllable types based on the morphology of the main component of the vocalization (**Figure 2.3.3A-B**) [30]. The output of the method was the probability for each USV to be of a certain syllable type. The highest probability (P_1) defined the syllable type for a given USV (**Figure 2.3.3A**). The percent use of each

syllable type per recording was compared between genotypes at each age using two-way ANOVA. Using this approach, we did not find any significant differences in the distribution of syllable types emitted by control and *Magel2*$^{m+/p-}$ mice at P6 (genotype: $F_{1, 374} = 2.5 \times 10^{-16}$, $P > 0.99$; class: $F_{10, 374} = 93.25$, $P < 10^{-4}$; genotype x class: $F_{10, 374} = 1.00$, $P = 0.44$) and P12 (genotype: $F_{1, 616} = 7.7 \times 10^{-16}$, $P > 0.99$; class: $F_{10, 616} = 278$, $P < 10^{-4}$; genotype x class: $F_{10, 616} = 0.81$, $P = 0.62$; **Figure 2.3.3C, 2.3.3F**). At P8, however, *Magel2*$^{m+/p-}$ pups emit vocalizations of different syllable types (genotype: $F_{1, 539} = 2.2 \times 10^{-15}$, $P > 0.99$; class: $F_{10, 539} = 167$, $P < 10^{-6}$; genotype x class: $F_{10, 539} = 9.51$, $P < 10^{-6}$; **Figure 2.3.2D)**, which include: 55% less USVs of the type *chevron* (control: 9.0 ± 1.6 %; *Magel2*$^{m+/p-}$: 4.0 ± 0.01 %; $P = 0.02$, Holm-Šídák test); 44% less USVs of the type *step-up* (control: 14.3 ± 1.4 %; *Magel2*$^{m+/p-}$: 8.1 ± 1.3 %; $P < 10^{-3}$, Holm-Šídák test); 36% more USVs of the type *flat* (control: 9.6 ± 0.9 %; *Magel2*$^{m+/p-}$: 15.2 ± 1.2 %; P = 0.007, Holm-Šídák test); and 33% more USVs of the type *short* compared to controls (control: 23.6 ± 1.8 %; *Magel2*$^{m+/p-}$: 35.5 ± 2.0 %; $P < 10^{-4}$, Holm-Šídák test; **Figure 2.3.3D)**. At P10, we also identified discrete differences in the emission of USVs of different syllable types between groups (genotype: $F_{1, 462} = 8.1 \times 10^{-17}$, $P > 0.99$; class: $F_{10, 462} = 149$, $P < 10^{-4}$; genotype x class: $F_{10, 462} = 2.11$, $P = 0.02$; **Figure 2.3.2E**): *Magel2*$^{m+/p-}$ pups emit 19% less *down frequency modulation* (control: 31.0 ± 2.1 %; *Magel2*$^{m+/p-}$: 25.0 ± 1.5 %; $P = 0.02$; Holm-Šídák test) and emit 53% more *up frequency modulation* (control: 4.8 ± 0.8 %; *Magel2*$^{m+/p-}$: 10.3 ± 2.0 %; $P = 0.04$; Holm-Šídák test; **Figure 2.3.3E**). (**Table S1** provides a detailed analysis of the spectro-temporal features of each syllable type across all ages tested in controls and *Magel2*$^{m+/p-}$ pups). In summary, we found that *Magel2*$^{m+/p-}$ mice at P8 use simpler vocalizations that fall under the 'flat' and 'short' classifications instead of multicomponent USVs. These findings are in line with our previous results **(Figures 3.2.1-2)** demonstrating that the largest differences in vocal behavior occur in eight-day-old *Magel2*$^{m+/p-}$ pups.

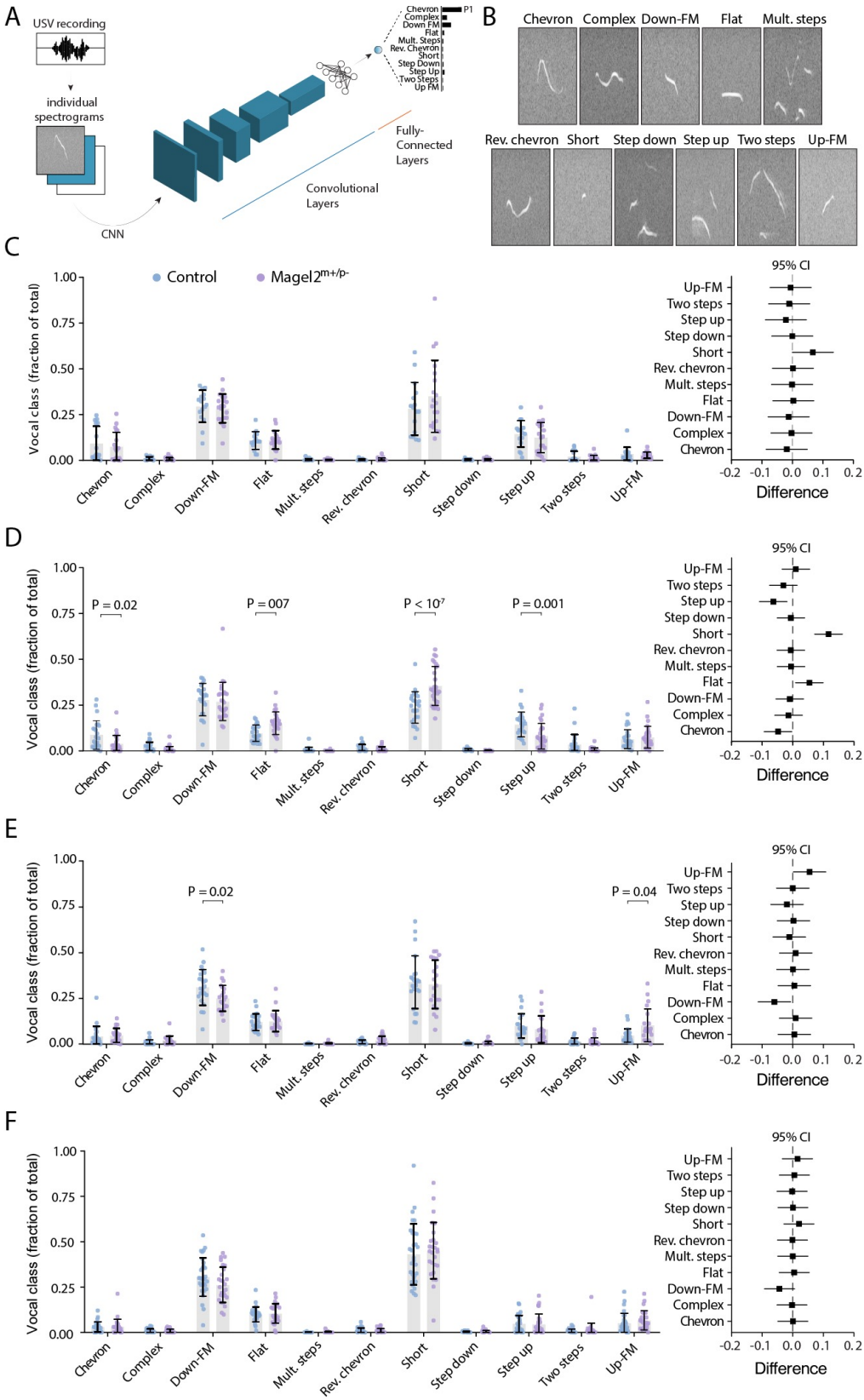
A
USV recording
individual spectrograms
CNN
Convolutional Layers
Fully-Connected Layers
Chevron
Complex
Down FM
Flat
Mult. Steps
Rev. Chevron
Short
Step Down
Step Up
Two Steps
Up FM
P1
B
Chevron
Complex
Down-FM
Flat
Mult. steps
Rev. chevron
Short
Step down
Step up
Two steps
Up-FM
C
Control
Magel2m+/p-
Vocal class (fraction of total)
95% CI
Difference
D
P = 0.02
P = 007
P < 10-7
P = 0.001
E
P = 0.02
P = 0.04
F

Figure 2.3.3 Magel2 deficiency alters USV class repertoire. *(**A**) Illustration of the convolutional neural network used to classify each USV into one of eleven syllable types based on their morphology in spectrograms. (**B**) Spectrograms representing each of the eleven syllable types. (**C**) Distribution of syllable types in P6 pups—control in blue and Magel2 deficient in purple. Data are showed as fraction of the total number of USVs; right panel denotes the 95% confidence intervals as a measure of effect size. (**D**) Similar to (C), but for P8 pups. (**E**) Similar to (C), but for P10 pups. (**F**) Similar to (C), but for P12 pups. Bars represent mean value with error bars representing SEM and round symbols representing individual values. When plotting the effect sizes, squared symbols and black lines represent 95% confidence intervals calculated as the different between Magel2 deficient and control pups. P values are provided in the figures as calculated using Sidak's multiple comparison test as a post hoc analysis after two-way ANOVA. The sample sizes for control and Magel2 deficient pups are: P6, n = 16 and 20; P8, n = 23 and 28; P10, n = 23 and 20; and P12, n = 30 and 28, respectively.*

2.3.4 Altered vocal repertoire of *Magel2*$^{m+/p-}$ mice

As stated above, the vocal analysis pipeline outputs the probability for each USV to be classified as each of the eleven syllable types (P_1, P_2, P_3, … $P_{11;}$ **Figure 2.3.3A-B**). This distribution of probabilities allows the qualitative and quantitative comparison of the vocal classification among groups[30]. By taking into account the distribution of probabilities to classify each USV, it is possible to estimate how similar the vocal repertoire of one group of mice is to another group. To compare the vocal repertoire of mice across all ages studied, we used diffusion maps—a dimensionality reduction technique that decreases the number of dimensions of the probability distribution from eleven classes to three dimensions in a Euclidean space (**Figure 2.3.4A**)[30]. Using pairwise comparisons (**Figure**

2.3.4B), we estimated the similarity between the vocal repertoire of mice of different ages and genotypes. Using this method, we found that control pups at P6 and P8 (Cohen's coefficient: $\kappa = 0.99$) and control pups at P10 and P12 (Cohen's coefficient: $\kappa = 0.95$) display vocal repertoires that are similar to each other (**Figure 2.3.4C-D**). These two age groups (P6-P8 and P10-P12), however, present lower pairwise similarities when compared to each other with κ ranging from 0.67 to 0.77 (**Figure 2.3.4E**). These results suggest that the vocal repertoire of control pups undergoes significant changes between P8 and P10.

Next, we analyzed the same transitions in the vocal repertoire of *Magel2*$^{m+/p-}$ pups. The comparison between the vocal repertoire of *Magel2*$^{m+/p-}$ pups at P6 and P8 show lower pairwise similarity ($\kappa = 0.80$) compared to control pups (**Figure 2.3.4F**). In contrast to littermate controls, *Magel2*$^{m+/p-}$ pups at P8 show a higher pairwise similarity with P10 ($\kappa = 0.84$) and P12 ($\kappa = 0.99$) pups (**Figure 2.3.4F-H)**. Finally, we directly compared the vocal repertoire of *Magel2*$^{m+/p-}$ and control pups. *Magel2*$^{m+/p-}$ pups, at P6, show high pairwise similarity when compared to controls at P6 ($\kappa = 1.00$) and P8 ($\kappa = 1.00$), but not at P10 ($\kappa = 0.80$) and P12 ($\kappa = 0.72$). At P8, *Magel2*$^{m+/p-}$ pups show relatively low pairwise similarities with control pups at P6 ($\kappa = 0.76$) and P8 ($\kappa = 0.78$) but show high similarities with control pups at P10 ($\kappa = 1.00$) and P12 ($\kappa = 0.95$). At P10, *Magel2*$^{m+/p-}$ pups show relatively lower pairwise similarities with control pups at P6 ($\kappa = 0.67$) and P8 ($\kappa = 0.70$) than at P10 ($\kappa = 0.82$) and P12 ($\kappa = 0.81$). This pattern is more evident in P12 Magel2$^{m+/p-}$ pups, which show lower pairwise similarities with control pups at P6 ($\kappa = 0.74$) and P8 ($\kappa = 0.75$) than at P10 ($\kappa = 0.99$) and P12 ($\kappa = 0.97$).

Altogether, these analyses suggest a different dynamic for the ontogeny of the vocal repertoire of *Magel2*$^{m+/p-}$ compared to control pups—with *Magel2*$^{m+/p-}$ pups at a younger

age (i.e., P8) resembling control pups at an older age (i.e., P10-P12). Thus, the period of development between P8 and P10 seems to mark an important period for the effect of the maternally imprinted gene, *Magel2*, on the vocal behavior of the offspring.

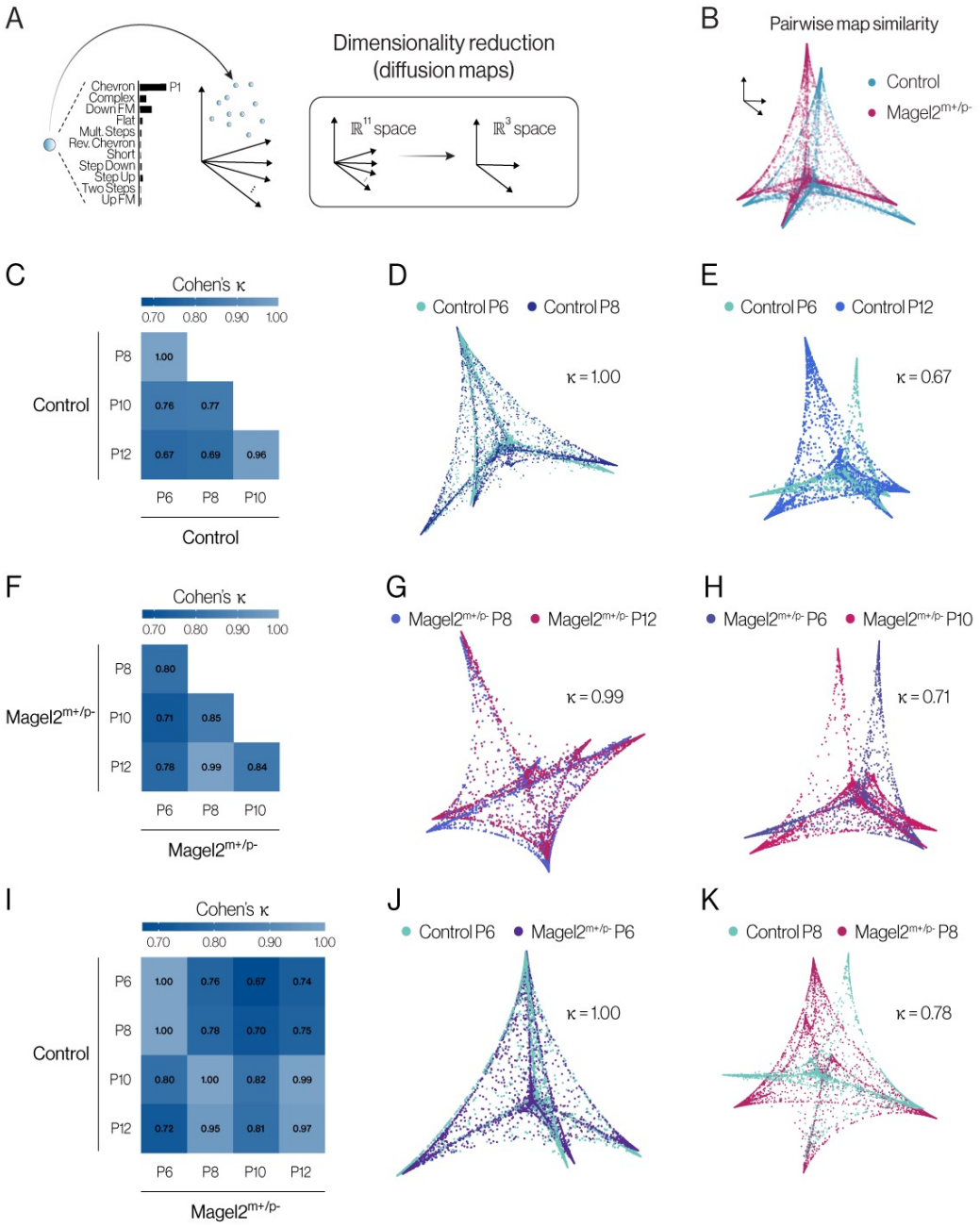

Figure 2.3.4 Magel2 deficiency shortens USV developmental traits. *(**A**) Illustration of the output of the convolutional neural network, with a distribution of eleven probabilities for vocal classification (one probability for each of the eleven syllable types, with the highest probability defining the syllable type). Using diffusion maps, a dimensionality reduction technique, these eleven dimensions are reduced to three dimensions in the Euclidian space. (**B**) Illustration of a pairwise comparison of the vocal repertoire of pups using diffusion maps and 3D alignment of the manifolds (see methods for more details). (**D**) Comparison of the pairwise distance matrix between control pups at different ages using Cohen's Kappa coefficient. (**D-E**) Examples of two pairwise comparisons with high and low alignment. (**F-H**) Similar to (**D-E**), but for Magel2 deficient pups. (**I-K**) Similar to (C-H), but comparing control and Magel2 deficient pups across ages. The sample sizes for control and Magel2 deficient pups are: P6, n = 16 and 20; P8, n = 23 and 28; P10, n = 23 and 20; and P12, n = 30 and 28, respectively.*

2.3.5 Dams show impaired retrieval behavior to *Magel2*$^{m+/p-}$ P8 pups

The emission of vocalization by infants draws caregiver's attention and care[25-27,31] while genetically mute mouse pups are neglected by their dams[40]. Together, these observations led us to speculate that the deficiency of *Magel2* in pups, which alters vocal behavior, could lead to altered maternal behavior. In order to test this idea, we used a behavior assay to quantify maternal behavior towards their own control and *Magel2*$^{m+/p-}$ offspring. In this assay, dams are first placed in the middle of a three-chamber apparatus that contains their home nest in the middle chamber (**Figure 2.3.5A**). After a period of acclimation, in the next stage, one pup of each genotype is placed at the opposite ends of the apparatus. The time (latency) to retrieve each pup back to the nest is then recorded (**Figure 2.3.5A**).

We initially evaluated whether dams show a preference to retrieve pups from one of the genotypes at postnatal day eight. This analysis shows that control pups were more likely to be retrieved first (11/15 trials; 73.3%) compared to *Magel2*$^{m+/p-}$ pups (4/15 trials; 26.7%; **Figure 2.3.5B and Table S2**). Accordingly, on average, the latency to retrieve control pups was less than half of the latency to retrieve *Magel2*$^{m+/p-}$ pups (control: 51.9 ± 12.9 s; *Magel2*$^{m+/p-}$: 104.6 ± 19.1 s; $W = 82$, $P_{2\text{-tail}} = 0.01$, Wilcoxon matched-pairs signed rank test; **Figure 2.3.5C**). Because eleven out of fifteen *Magel2*$^{m+/p-}$ pups were retrieved second, we also ran experiments placing wildtype control pups in both ends of the apparatus to compare the latency to retrieve the second pup in each of the experiments. Using this comparison, dams took twice as long to retrieve *Magel2*$^{m+/p-}$ pups compared to control pups (control: 64.57 ± 12.3 s; *Magel2*$^{m+/p-}$: 126.3 ± 22.23 s; $t_{14.86} = 2.21$, $P_{2\text{-tail}} = 0.04$, Welch's *t* test; **Figure 2.3.5D**)**.** We also performed similar experiments with pups at postnatal day six and did not find significant differences in maternal retrieval behavior (**Figure 2.7.4**). In summary, the deficiency of Magel2 in offspring alters not only offspring behavior but also the behavior of the mother towards their own offspring.

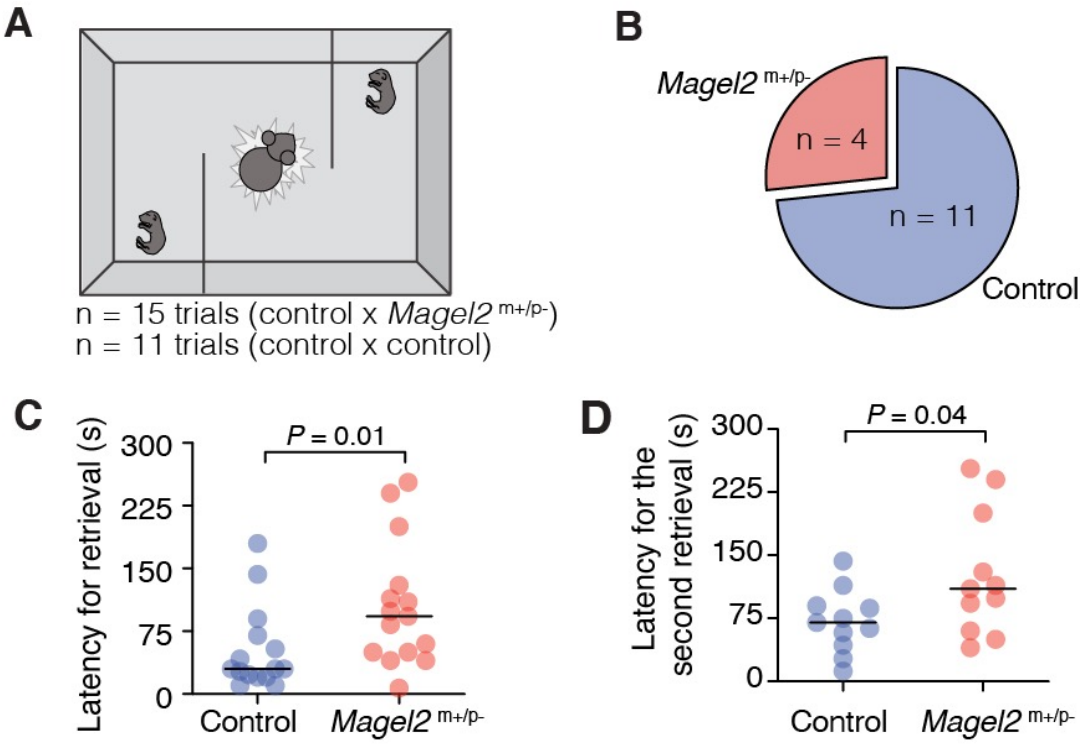

Figure 2.3.5. Magel2 deficiency affects maternal retrieval behavior. *(**A**) Diagram of maternal retrieval protocol with P8 pups on opposite ends of the apparatus and mother at nest in the middle compartment. (**B**) Pie chart showing the proportion of pups of each genotype that were retrieved first by the dam in the test (n = 15 trials testing control versus Magel2 deficient pup). (**C**) Latency for the dam to retrieve control and Magel2 deficient pups. (**D**) Latency for the dam to retrieve the second pup in the test (the total number of control pups is n = 11, which represents the 7 pups retrieved second in the control versus control trials plus the 4 pups retrieved second in the control versus Magel2 deficient pup trials). Significant P values are shown in the graphs.*

2.4 Discussion

In this study, we recorded and analyzed vocalizations from *Magel2* deficient pups and their wildtype littermates at postnatal days 6, 8, 10 and 12. Using custom-built software to automatically quantify vocalizations[30], we counted the number of vocalizations and measured the spectro-temporal features of each vocalization, including its intensity, duration, bandwidth, mean frequency, maximum frequency, minimum frequency, and use of harmonic components. We also assigned a syllable type for each vocalization based on its morphological features in the time-frequency plane. We used further quantitative methods to analyze the vocal repertoire of mice across groups and ages. These methods shed light on discrete changes in the development of separation-induced vocalizations in *Magel2* deficient mice that are more pronounced at postnatal day eight.

With regard to the vocal behavior of wildtype mice, our results demonstrate that the emission of separation-induced USVs gradually decreases from P6-P8 to P10-P12. This result agrees with previous studies, which show an inverse-U shape profile for separation-induced vocalizations in mice during the first two weeks of life[22,23,29]. Moreover, we found that wildtype mice use simpler vocalizations at older ages (P10-P12) compared to younger ages (P6-P8). These findings in wildtype mice provide the basis for comparisons with *Magel2* deficient pups.

Magel2 deficient pups show different dynamics for separation-induced vocalizations. At P6, these pups vocalize comparably to wildtype littermates, but at P8, their vocal number and features resemble wildtype littermates that are older (P10-P12). The sex of the pups

and their body temperature at the end of the test could not explain these differences. An explanation for these results is that *Magel2* deficient pups are less responsive to certain social cues. In socially isolated pups, therefore, the deprivation of these cues would not induce the behavior to the same degree as in wildtype pups. An alternative explanation for these results is that for *Magel2* deficient pups, vocal behavior does not have the same fitness value compared to wildtype pups. In the latter case, the behavior begins to change at younger ages due to the lack of reinforcement (maternal care). While it is difficult to prove these interpretations experimentally, the delayed latency for dams to retrieve *Magel2* deficient pups at P8 compared to wildtype littermates supports the idea that the deficiency of this imprinted gene impairs the fitness of the offspring. Moreover, the fact that *Magel2* deficient pups have lower body mass during early development further suggests a decrease in the fitness of these animals. Whether the change in vocal behavior and the decrease in body mass and maternal behavior are causally related warrants further investigation.

Interestingly, the deficiency of *Magel2* is not the only example of an imprinted gene affecting the emission of USVs by mouse pups. Consider, for example, previous studies of other imprinted genes. Deletion of the paternally inherited imprinted gene *Peg3* lowers vocal rate in mouse pups[9]. Moreover, duplication of the paternal imprint loci on chromosome 15 increases the separation-induced vocalization of mouse pups[41]. Conversely, deletion of the maternally inherited genes *Gabrb3* and *Ube3a* increases vocal rate[13]. Deletion of Mecp2, which regulates Ube3a expression, also leads to a dramatic increase in USV emission[42]. Although not related, mutations in the X chromosome also led to similar changes in USV phenotypes. Autism Mouse Model MALTT has a mutation in a non-coding region in the X chromosome; these mice emit more USVs from postnatal day 8-13[43]. Based on these findings, it is tempting to

speculate that imprinted genes inherited from the father increase vocal rate while imprinted genes inherited from the mother decrease vocal rate. To test this generalization more formally, future studies will need to test the effect of *all* imprinted genes on the vocal behavior of the offspring.

Magel2$^{m+/p-}$ pups at P8 vocalize at a lower rate compared to their littermate controls, mainly emitting short and flat vocals similar to those of older pups. Moreover, when we estimate the similarity between the vocal repertoire of mutant and wildtype pups across ages tested, we find that, at P8, *Magel2*$^{m+/p-}$ pups emit USVs that are most similar to those produced by wildtype pups at P10 and P12. The reason for the specific change in vocal behavior at postnatal day 8 is not known. Further studies are necessary to describe whether deviation in USV emission for *Magel2* deficient mice represents some kind of curve shift in the behavior. For example, it could be that the critical phase in which pups use separation-induced vocalization to gain maternal attention is shortened in offspring deficient for *Magel2.* Interestingly, reduction in USV rate is commonly found in animal models of autism spectrum disorder—a neurodevelopmental disorder highly comorbid with MAGEL2$^{m+/p-}$ patients[16]—that also present deficits in social behavior. Thus, our findings suggest that alteration in the emission of USVs is part of a social behavior deficit in *Magel2*$^{m+/p-}$ pups that continues into adulthood[20,26,41].

Two methodological aspects of this study are important to highlight. First, the emission of separation induced USVs was measured after postnatal day six, disregarding the analysis of this behavior at younger ages. This age was chosen, however, because at younger ages mouse pups cannot maintain their body temperature[44], adding an additional stressor and confounder to the measurements of vocal behavior. Second, the emission of USVs was recorded for 20 minutes, which provides robust power to the

analysis of vocal behavior due to the high number of USVs recorded. However, this period of recording is substantially longer than what has been typically used in the past, with separation protocols ranging from 3-5 minutes[23,37]. Thus, this prolonged separation could add an additional stressor to the pups that could potentially alter the results. Three lines of evidence, however, suggest otherwise: (1) Data analyzed in 5-minute bins show the same changes in the rate of vocalizations as the data analyzed for the total of the 20 minutes. (2) Prolonged separation of up to 90 minutes does not trigger a hypothalamic-pituitary axis response, with pups showing no increase in corticosterone levels [39]. (3) Testing pups only one or repeatedly did not alter the vocal behavior (Figure 2.7.3). Thus, the additional time of recording used in this study does not seem to significantly affect the behavior of the pups, while adding more power to the analysis of this behavior.

In broader terms, we posit that our findings support the theory that genomic imprinting evolved to balance the cost of the phenotype for the offspring and for the mother, as well as to balance the best interests of mothers and fathers in altering offspring's phenotype[6,7]. In the case of paternally inherited genes, the expression of these genes increases vocal behavior, thus, increasing maternal care and favoring the use of maternal resources, which is in the best interests of the father. Conversely, the loss of these paternally inherited genes decreases vocal behavior and, consequently, the demand for maternal care, thus, conserving maternal resources, which is in the best interests of the mother[2,6,7]. This theoretical framework is supported by our findings in a test that measures the latency to retrieve isolated pups back to the home nest, which demonstrate impaired maternal care towards Magel2 deficient pups compared to wildtype littermates[2,9,40]. As alluded above, future studies should test this theoretical view more directly by systematically investigating the effect of imprinted genes on the behavior of offspring and on the behavior of mothers towards their offspring. These

efforts will help elucidate behavior phenotypes that occur in neurodevelopmental disorders as well as expand our understanding of the evolutionary adaptation of genomic imprinting.

2.5 Material and Methods

2.5.1 Experimental models and subject details

All preweaning mice used in the experiments were 6 to 12 days old from both sexes. Litters were provided from 9 separate breeding pairs. Separate litters were used for isolation and maternal retrieval tests (for further details **Table S1 and S2)**. Dams used were 2 to 6 months old. To generate experimental pups, we used the following cross: *Magel2*$^{m+/p-}$ (Jax #009062) dams bred with C57BL/6J (Jax #000664) males. Offspring from this cross were either *Magel2*$^{m+/p-}$ or wildtype (*Magel2*$^{m+/p+}$). All mice were kept in temperature- and humidity-controlled rooms, in a 12/12 hr. light/dark cycle, with lights on from 7:00 AM–7:00 PM. Studies took place during the light cycle. Food (Teklad 2018S, Envigo) and water were provided ad libitum. All procedures were approved by IACUC (Yale University).

2.5.2 Separation-induced vocalization

Pups from the same litter were placed individually in a soundproof chamber containing fresh bedding material[23,39]. An UltraSoundGate Condenser Microphone CM 16 (Avisoft Bioacoustics, Berlin, Germany) was placed 10 cm above the recording chamber and connected to the UltraSoundGate 416 USGH device to record ultrasonic vocalizations. The recording sessions lasted 20 minutes. Four to eight chambers were recorded simultaneously. After testing, mice were placed back in their home cage with the dam. Pups were tested at postnatal days 6, 8, 10, and 12. The number of audio recordings per

age and per sex were as follows: control [P6 (female, n = 9; male, n = 7), P8 (female, n = 14; male, n = 9), P10 (female, n = 10; male, n = 13), and P12 (female, n = 15; male, n = 15)] and *Magel2*$^{m+/p-}$ [P6 (female, n = 10; male, n = 10), P8 (female, n = 15; male, n = 13), P10 (female, n = 11; male, n = 9), and P12 (female, n = 16; male, n = 12)]. Because pups that were naïve for the test—only tested at one specific age—show similar results as pups tested at multiple ages (**Figure S3**, similar to previous findings [45,46]), we pooled all mice together for our analysis.

2.5.3 Vocalization analysis

Ultrasonic vocalizations were automatically extracted from audio recordings using a custom-built tool[30]. We measured USVs that occurred above 45 kHz, as in our laboratory we only find very rare USVs in the 30-45 kHz range. We manually validated 32 audio recordings in this study to identify USVs within the 30-45 kHz range and found a median of 0% (and a mean of 0.15%) USVs per recording with a 95% CI of [0, 0.23] (in %). Due to the rarity of these USVs and the added difficulty of identifying them using automated tools because of audible noise that projects into the ultrasonic space, we did not consider in our analysis USVs that occurred below 45 kHz. In brief, audio recordings were converted from the time-domain to the frequency-domain using a 1024-point Fast Fourier Transform (FFT) through a 512-width hamming window with 50% overlap. Spectrograms were computed from the FFT and processed as images. Each pixel in the spectrogram corresponded to the intensity of each time-frequency component. Next, we applied a series of image-processing techniques (e.g., contrast enhancement, binarization, median filter, and morphological operations) to obtain segmentation of candidate vocalizations. A single spectrogram was generated for each candidate vocalization detected. Candidate vocalizations were classified as noise or real vocalization using a local median noise filter. The remaining vocalization candidates are

further labeled under one of eleven call type classifications[28,30,39] using a Convolutional Neural Network (CNN), or as noise. The CNN was trained using a curated vocalization dataset, containing over 20,000 noise samples and 40,000 vocalization samples. Finally, the tool produces one spectrogram centralized on each vocalization for visual inspection, and a table (*xlsx* format) containing spectral features for each USV, such as time, duration, bandwidth, frequency, and intensity (minimum, mean, and maximum) values.

2.5.4 Temperature measurements

In some trials, surface body temperature was recorded after the 20-minute isolation period using infrared thermography. Briefly, pups were recorded using an infrared thermal camera (FLIR T450, FLIR Systems, Oregon, U.S.) positioned 20 cm above the chamber for a period of 30 seconds. The body temperature was calculated by integrating the maximum temperature measured at each frame of the 30 seconds recording.

2.5.5 Maternal Retrieval Test

The maternal preference test was performed in a three-chamber apparatus (65 x 42 x 23 cm) and comprised of three stages: Stage 1 – acclimation: the dam was allowed to explore the apparatus without the presence of pups for five minutes. In the middle of the apparatus, home cage nesting under an infrared igloo. Stage 2 – exploration: two P8 mice were placed on each side of the apparatus and the dam was allowed to explore the pups for five minutes. Stage 3 - preference: dam was recorded while she retrieved pups back to her home cage nesting. Groups were randomly alternated between both sides to avoid preference for one side of the chamber. Latency to retrieve each pup was timed from videos taken of the retrieval tests. Summary of results found in **Table S2**.

2.5.6 Quantification and statistical analysis

Prism 8.0 or above was used to analyze data and plot figures. Shapiro-Wilk normality test was used to assess normal distribution of the data. To analyze differences in the use of harmonics, we used the non-parametric Mann-Whitney Test with Bonferroni correction to find statistically different effects. Comparison of diffusion maps were analyzed through pairwise comparison using Cohen's kappa coefficient. Maternal retrieval latency for retrieval of each pup from the start of test used Wilcoxon test. Analysis of second retrieval latency from first retrieval was calculated using Welch's t test. The rest of the data was analyzed using two-way ANOVA or mixed-effects analysis. Sidak's multiple comparisons test was used to find post hoc differences among groups and to calculate the 95% confidence intervals to report effect size. In the text, values are provided as mean ± SEM. $P < 0.05$ was considered statistically significant and, when necessary and as described above, was corrected using Bonferroni's method. Statistical data are provided in text and in the figures.

2.8 References

1. Barlow DP, Bartolomei MS. Genomic imprinting in mammals. *Cold Spring Harb Perspect Biol.* 2014;6(2).
2. Perez JD, Rubinstein ND, Dulac C. New Perspectives on Genomic Imprinting, an Essential and Multifaceted Mode of Epigenetic Control in the Developing and Adult Brain. *Annu Rev Neurosci.* 2016;39:347-384.
3. Ferguson-Smith AC. Genomic imprinting: the emergence of an epigenetic paradigm. *Nat Rev Genet.* 2011;12(8):565-575.
4. Morison IM, Ramsay JP, Spencer HG. A census of mammalian imprinting. *Trends Genet.* 2005;21(8):457-465.
5. Haig D. Coadaptation and conflict, misconception and muddle, in the evolution of genomic imprinting. *Heredity (Edinb).* 2014;113(2):96-103.
6. Patten MM, Ross L, Curley JP, Queller DC, Bonduriansky R, Wolf JB. The evolution of genomic imprinting: theories, predictions and empirical tests. *Heredity (Edinb).* 2014;113(2):119-128.
7. Spencer HG, Clark AG. Non-conflict theories for the evolution of genomic imprinting. *Heredity (Edinb).* 2014;113(2):112-118.
8. Bervini S, Herzog H. Mouse models of Prader-Willi Syndrome: a systematic review. *Front Neuroendocrinol.* 2013;34(2):107-119.
9. Li L, Keverne EB, Aparicio SA, Ishino F, Barton SC, Surani MA. Regulation of maternal behavior and offspring growth by paternally expressed Peg3. *Science.* 1999;284(5412):330-333.

10. Bischof JM, Stewart CL, Wevrick R. Inactivation of the mouse Magel2 gene results in growth abnormalities similar to Prader-Willi syndrome. *Hum Mol Genet.* 2007;16(22):2713-2719.

11. Martinez ME, Charalambous M, Saferali A, et al. Genomic imprinting variations in the mouse type 3 deiodinase gene between tissues and brain regions. *Mol Endocrinol.* 2014;28(11):1875-1886.

12. Hernandez A, Martinez ME, Fiering S, Galton VA, St Germain D. Type 3 deiodinase is critical for the maturation and function of the thyroid axis. *J Clin Invest.* 2006;116(2):476-484.

13. Jiang YH, Pan Y, Zhu L, et al. Altered ultrasonic vocalization and impaired learning and memory in Angelman syndrome mouse model with a large maternal deletion from Ube3a to Gabrb3. *PLoS One.* 2010;5(8):e12278.

14. Angulo MA, Butler MG, Cataletto ME. Prader-Willi syndrome: a review of clinical, genetic, and endocrine findings. *J Endocrinol Invest.* 2015;38(12):1249-1263.

15. Nicholls RD, Knoll JH, Butler MG, Karam S, Lalande M. Genetic imprinting suggested by maternal heterodisomy in nondeletion Prader-Willi syndrome. *Nature.* 1989;342(6247):281-285.

16. Bennett JA, Germani T, Haqq AM, Zwaigenbaum L. Autism spectrum disorder in Prader-Willi syndrome: A systematic review. *Am J Med Genet A.* 2015;167A(12):2936-2944.

17. Kong X, Zhu J, Tian R, et al. Early Screening and Risk Factors of Autism Spectrum Disorder in a Large Cohort of Chinese Patients With Prader-Willi Syndrome. *Front Psychiatry.* 2020;11:594934.

18. Schaaf CP, Gonzalez-Garay ML, Xia F, et al. Truncating mutations of MAGEL2 cause Prader-Willi phenotypes and autism. *Nat Genet.* 2013;45(11):1405-1408.

19. Thomason MM, McCarthy J, Goin-Kochel RP, Dowell LR, Schaaf CP, Berry LN. Neurocognitive and Neurobehavioral Phenotype of Youth with Schaaf-Yang Syndrome. *J Autism Dev Disord.* 2020;50(7):2491-2500.

20. Fountain MD, Tao H, Chen CA, Yin J, Schaaf CP. Magel2 knockout mice manifest altered social phenotypes and a deficit in preference for social novelty. *Genes Brain Behav.* 2017;16(6):592-600.

21. Branchi I, Santucci D, Alleva E. Ultrasonic vocalisation emitted by infant rodents: a tool for assessment of neurobehavioural development. *Behav Brain Res.* 2001;125(1-2):49-56.

22. Hofer MA, Shair HN, Brunelli SA. Ultrasonic vocalizations in rat and mouse pups. *Curr Protoc Neurosci.* 2002;Chapter 8:Unit 8 14.

23. Shair HN. Acquisition and expression of a socially mediated separation response. *Behav Brain Res.* 2007;182(2):180-192.

24. Noirot E. Ultrasounds and maternal behavior in small rodents. *Dev Psychobiol.* 1972;5(4):371-387.

25. Panksepp J, Normansell L, Herman B, Bishop P, Crepeau L. Neural and Neurochemical Control of the Separation Distress Call. In: Newman JD, ed. *The Physiological Control of Mammalian Vocalization.* Boston, MA: Springer US; 1988:263-299.

26. Wohr M, Schwarting RK. Maternal care, isolation-induced infant ultrasonic calling, and their relations to adult anxiety-related behavior in the rat. *Behav Neurosci.* 2008;122(2):310-330.

27. Portfors CV, Perkel DJ. The role of ultrasonic vocalizations in mouse communication. *Curr Opin Neurobiol.* 2014;28:115-120.

28. Grimsley JM, Monaghan JJ, Wenstrup JJ. Development of social vocalizations in mice. *PLoS One.* 2011;6(3):e17460.

29. Branchi I, Santucci D, Alleva E. Analysis of ultrasonic vocalizations emitted by infant rodents. *Curr Protoc Toxicol.* 2006;Chapter 13:Unit13 12.

30. Fonseca AH, Santana GM, Bosque Ortiz GM, Bampi S, Dietrich MO. Analysis of ultrasonic vocalizations from mice using computer vision and machine learning. *Elife.* 2021;10.

31. Hahn ME, Lavooy MJ. A review of the methods of studies on infant ultrasound production and maternal retrieval in small rodents. *Behav Genet.* 2005;35(1):31-52.

32. Kamaludin AA, Smolarchuk C, Bischof JM, et al. Muscle dysfunction caused by loss of Magel2 in a mouse model of Prader-Willi and Schaaf-Yang syndromes. *Hum Mol Genet.* 2016;25(17):3798-3809.

33. Riede T. Subglottal pressure, tracheal airflow, and intrinsic laryngeal muscle activity during rat ultrasound vocalization. *J Neurophysiol.* 2011;106(5):2580-2592.

34. Allin JT, Banks EM. Effects of temperature on ultrasound production by infant albino rats. *Dev Psychobiol.* 1971;4(2):149-156.

35. Blumberg MS, Alberts JR. Ultrasonic vocalizations by rat pups in the cold: an acoustic by-product of laryngeal braking? *Behav Neurosci.* 1990;104(5):808-817.

36. Young DM, Schenk AK, Yang SB, Jan YN, Jan LY. Altered ultrasonic vocalizations in a tuberous sclerosis mouse model of autism. *Proc Natl Acad Sci U S A.* 2010;107(24):11074-11079.

37. Caruso A, Ricceri L, Scattoni ML. Ultrasonic vocalizations as a fundamental tool for early and adult behavioral phenotyping of Autism Spectrum Disorder rodent models. *Neurosci Biobehav Rev.* 2020;116:31-43.

38. Scattoni ML, Gandhy SU, Ricceri L, Crawley JN. Unusual repertoire of vocalizations in the BTBR T+tf/J mouse model of autism. *PLoS One.* 2008;3(8):e3067.

39. Zimmer MR, Fonseca AHO, Iyilikci O, Pra RD, Dietrich MO. Functional Ontogeny of Hypothalamic Agrp Neurons in Neonatal Mouse Behaviors. *Cell.* 2019;178(1):44-59 e47.

40. Hernandez-Miranda LR, Ruffault PL, Bouvier JC, et al. Genetic identification of a hindbrain nucleus essential for innate vocalization. *Proc Natl Acad Sci U S A.* 2017;114(30):8095-8100.

41. Nakatani J, Tamada K, Hatanaka F, et al. Abnormal behavior in a chromosome-engineered mouse model for human 15q11-13 duplication seen in autism. *Cell.* 2009;137(7):1235-1246.

42. Picker JD, Yang R, Ricceri L, Berger-Sweeney J. An altered neonatal behavioral phenotype in Mecp2 mutant mice. *Neuroreport.* 2006;17(5):541-544.

43. Hamilton SM, Spencer CM, Harrison WR, et al. Multiple autism-like behaviors in a novel transgenic mouse model. *Behav Brain Res.* 2011;218(1):29-41.

44. Kromkhun P, Katou M, Hashimoto H, Terada M, Moon C, Saito TR. Quantitative and qualitative analysis of rat pup ultrasonic vocalization sounds induced by a hypothermic stimulus. *Lab Anim Res.* 2013;29(2):77-83.

45. Barnes TD, Rieger MA, Dougherty JD, Holy TE. Group and Individual Variability in Mouse Pup Isolation Calls Recorded on the Same Day Show Stability. *Front Behav Neurosci.* 2017;11:243.

46. Verjat A, Rodel HG, Feron C. Isolation calls in house mouse pups: Individual consistency across time and situations. *Dev Psychobiol.* 2019;61(8):1135-1145.

2.7 Supplemental Figures

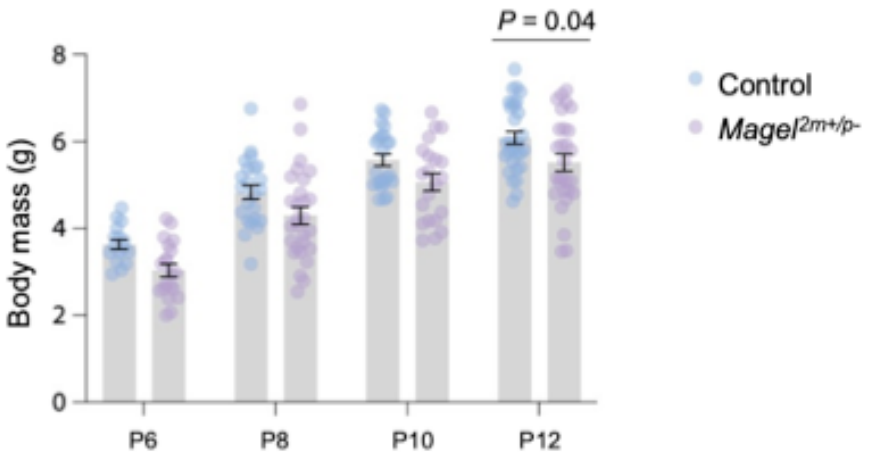

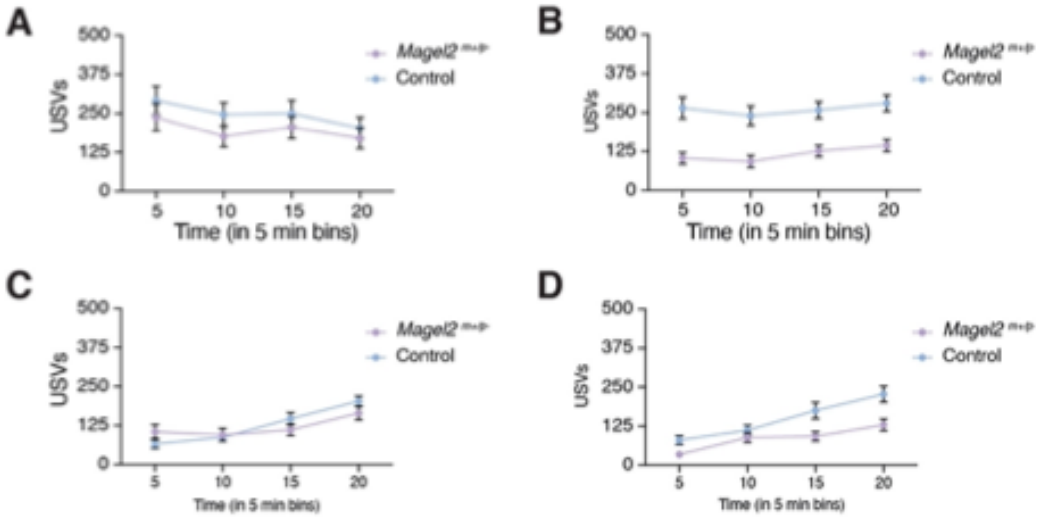

E

AGE	ANOVA table	F (DFn, DFd)	P value
P6	Interaction	F (3, 136)	0.97
	Time	F (3, 136)	0.23
	Genotype	F (1, 136)	0.06
P8	Interaction	F (3, 196)	0.93
	Time	F (3, 196)	0.29
	Genotype	F (1, 196)	4×10^{-15}
P10	Interaction	F (3, 164)	0.1
	Time	F (3, 164)	10^{-7}
	Genotype	F (1, 164)	0.59
P12	Interaction	F (3, 224)	0.17
	Time	F (3, 224)	5×10^{-9}
	Genotype	F (1, 224)	4×10^{-6}

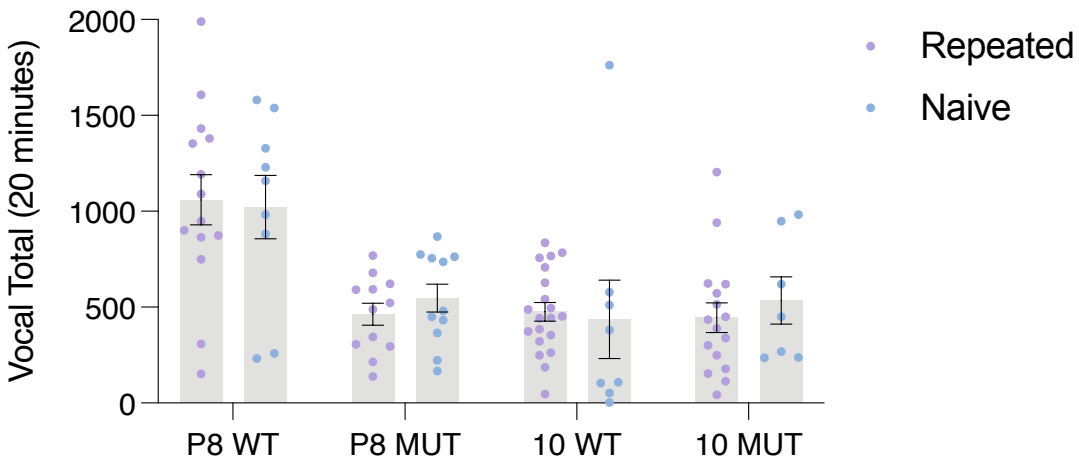
Vocal Total (20 minutes)
2000
1500
1000
500
0
P8 WT
P8 MUT
10 WT
10 MUT
Repeated
Naive

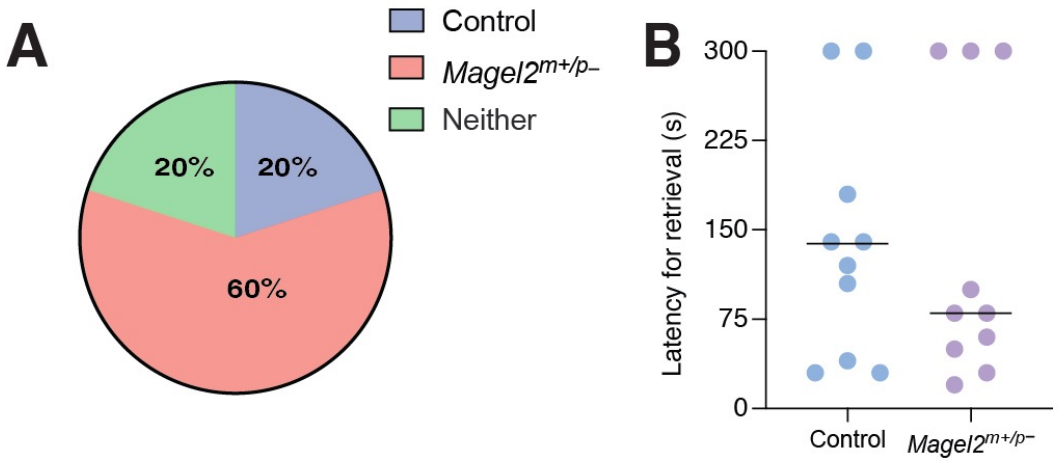
A
Control
Magel2m+/p–
Neither
20%
20%
60%
B
Latency for retrieval (s)
300
225
150
75
0
Control
Magel2m+/p–

Figure 2.7.1. Body mass of pups across tested ages. Individual body mass of control (blue) and *MageI2* deficient (purple) littermates at P6, P8, P10, and P12. Line with error bars represent mean and SEM. Round symbols representing individual values. *P* values are provided in the main text. The sample sizes for control and *MageI2* deficient pups are: P6, n = 16 and 20; P8, n = 23 and 28; P10, n = 23 and 20; and P12, n = 30 and 28, respectively.

Figure 2.7.2. Analysis of the emission of USVs in 5 minutes intervals from P6 to P12. Average USV emission of control (blue) and *MageI2* deficient (purple) littermates at (A) P6, (B) P8, (C) P10, and (D) P12. Symbols and error bars represent mean ± SEM. The results from two-way ANOVA with time as a repeated measure are provided in table (E). The sample sizes for control and *MageI2* deficient pups are: P6, n = 16 and 20; P8, n = 23 and 28; P10, n = 23 and 20; and P12, n = 30 and 28, respectively.

Figure 2.7.3. USV rate in naïve vs. experienced pups. Average USV emission of pups tested repeatedly (purple) and naïve pups (blue). Bars represent USV means for each genotype and condition. Line with error bars represent mean and SEM. Round symbols represent rate for individual pups. Multiple Mann-Whitney test was used to compare rates. *P* values are the following: P8 WT = 0.36; P8 MUT = 0.46; P10 WT = 0.46; P10 MUT = 0.58.

Figure 2.7.4. Maternal retrieval behavior of P6 pups. (**A**) Pie chart showing percentages of first retrieval of control and *MageI2* deficient pups from all trials. (**B**) Welch's t-test comparing the retrieval latency of control and *MageI2* deficient pups (no significant differences reported). The number of trials was n = 10.

A

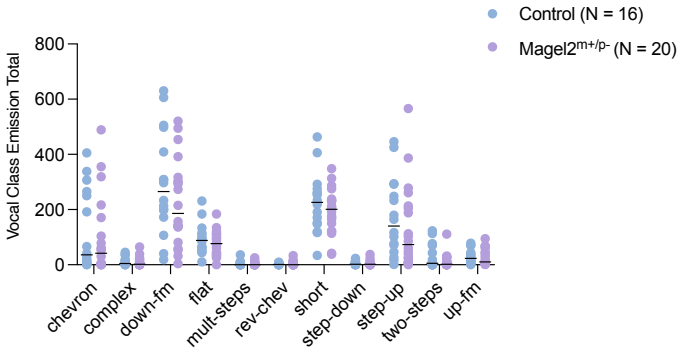
Control (N = 16)
Magel2m+/p- (N = 20)
Vocal Class Emission Total
800
600
400
200
0
chevron
complex
down-fm
flat
mult-steps
rev-chev
short
step-down
step-up
two-steps
up-fm

B

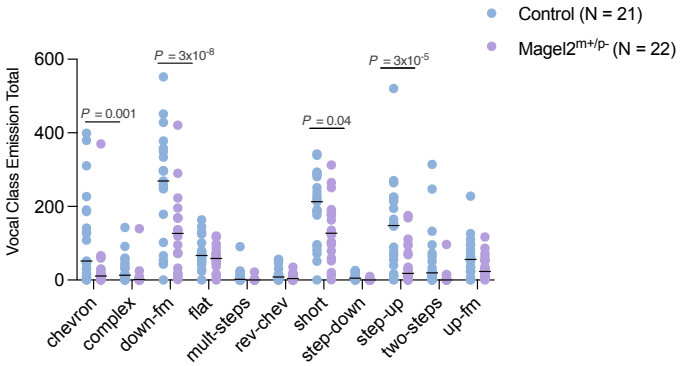
Control (N = 21)
Magel2m+/p- (N = 22)
Vocal Class Emission Total
P = 3x10-8
P = 3x10-5
P = 0.001
P = 0.04
600
400
200
0
chevron
complex
down-fm
flat
mult-steps
rev-chev
short
step-down
step-up
two-steps
up-fm

C

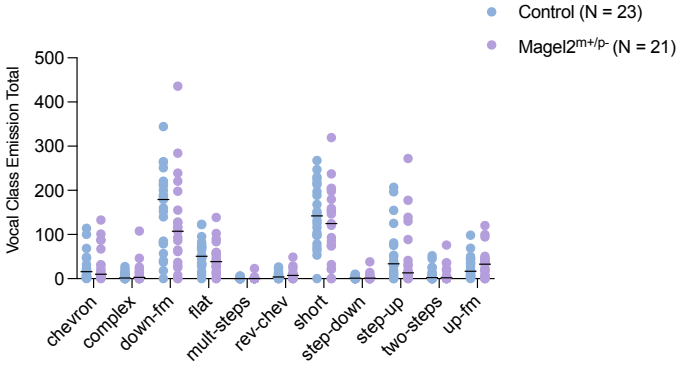
Control (N = 23)
Magel2m+/p- (N = 21)
Vocal Class Emission Total
500
400
300
200
100
0
chevron
complex
down-fm
flat
mult-steps
rev-chev
short
step-down
step-up
two-steps
up-fm

D

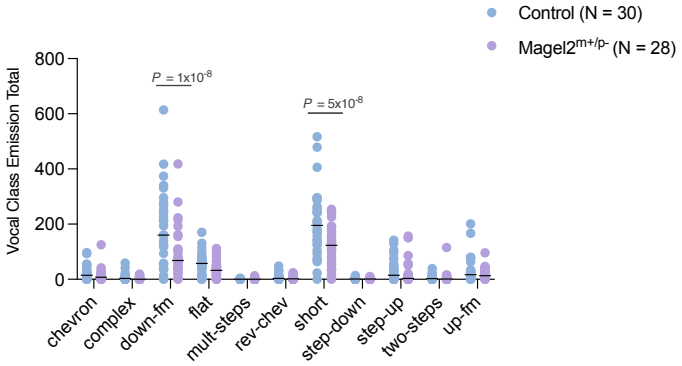
Control (N = 30)
Magel2m+/p- (N = 28)
Vocal Class Emission Total
P = 1x10-8
P = 5x10-8
800
600
400
200
0
chevron
complex
down-fm
flat
mult-steps
rev-chev
short
step-down
step-up
two-steps
up-fm

Figure 2.7.5 Total USV count per vocal class across ages *(**A**) Distribution of syllable types in (A) P6, (B) P8, (C) P10, (D) P12 pups. Control values are in blue and Magel2 deficient in purple. Values show total count of USVs done for each pup tested under both groups. Bars represent mean value with error bars representing SEM and round symbols representing individual values. P values are provided in the figures as calculated using Sidak's multiple comparison test as a post hoc analysis after two-way ANOVA. The sample sizes for control and Magel2 deficient pups are: P6, n = 16 and 20; P8, n = 23 and 28; P10, n = 23 and 20; and P12, n = 30 and 28, respectively.*

Chapter 3: Hypothalamic POMC neurons and β-endorphin modulate infant isolation-induced vocalizations

3.1 Abstract

Vocalization is important for infant mammal survival. In their first two weeks of life, mice are known to produce ultrasonic vocalizations (USV) whenever they are in isolation. During prolonged isolation, vocal rate drops. The mechanisms modulating this early behavior is not well understood. Our study suggests that infant mice drop USV after prolonged isolation as a consequence of β-Endorphin release from hypothalamic POMC neurons. Moreover, this hypothalamic POMC pathway may be part of the brain's response to distressed-induced pain, by inducing behavioral despair. Our results fill gaps in Panksepp's theory of endogenous opioids modulating affective states. Additionally, our findings give further evidence to the role of MOR endogenous opioids in social behavior. Here we share our experimental findings using genetic, chemogenetic and pharmacogenetic approaches. Our results broaden current understanding of affective behavior in early mammalian life.

3.2 Introduction

The nervous system allows animals to interact and respond to their environment. Through the senses, animals are able to discriminate between rewarding or aversive stimuli and behave accordingly. For example, the perception of pain following exposure to noxious or potentially noxious stimuli acts as a protective mechanism[1-3]. Part of the perception of pain is modulated by the central nervous system (CNS), which coordinates a series of physiological and behavioral responses as a way to maintain the organism in

optimal shape. In the case of pain, for example, the nervous system can activate pathways to ameliorate pain[1,4,5].

Importantly, pain is not just a consequence of physical harm, but also from negative affective states, such as stress and distress[3,6,7]. An example of a negative affective response to distress can be seen in mammalian infants. When infants find themselves in a situation of distress or discomfort, for example during separation from their caregivers, they cry or vocalize to attract caregiver nurture[8,9]. In some species, mere displacement from their home nest is enough to induce infant vocalizations[10,11]. These infant vocalizations are also referred to as *isolation-induced vocalizations* or *distress vocalizations*[8,12]. These distress vocalizations are thought to be modulated by the endogenous opioid system: Injection of morphine—an opioid receptor agonist—reduces infant vocalization, while naloxone—an opioid receptor antagonist—increases vocalizations[10,13]. These findings have been replicated in a variety of species, guinea pigs[3,14], chicks[14], rhesus macaque[15], and rodents[16].

In further support for the role of endogenous opioids on distress vocalizations, mice pups lacking μ-opioid receptors (MOR) show reduced vocalizations[17]. The principal endogenous ligand for MOR is β-endorphin[18,19]. β-endorphin is produced and released by cells that express the pro-opiomelanocortin peptide (POMC)[18,19]. POMC-producing cells reside in the pituitary gland, in the brainstem Nuleus Tract Solitarus (NTS), and in the arcuate nucleus of the hypothalamus (hereafter, I will call the neurons that produce POMC in the arcuate nucleus, $POMC^{ARC}$)[18,20]. POMC cells in the pituitary produce β-endorphin and is the primary source for peripheral nervous system (PNS)[21-23]. β-endorphin circulating in the CNS is thought to originate from the NTS or ARC. NTS has a small population of POMC neurons that project to overlapping targets as those in ARC.

Furthermore, most β-endorphin produced in the brain originates from the large populations of POMC neurons in ARC [21-23].

$POMC^{ARC}$ neurons seem to play important roles in pain sensitivity in adult mice. CNS pain modulation response depends on the nature of the stressor. For example, physical restraint, but not predator odor, activates $POMC^{ARC}$ neurons[24]; this is part of the descending pain pathway described above[1]. In this case, stress-induced $POMC^{ARC}$ activation produces an inhibitory tone downstream that manifest as despair behavior. Despair behavior is characterized by submission, anhedonia, and immobility[7,25,26]. Here, despair was measured by latency in trying to escape from standing on a hot plate. In other words, after restraint, mice spent longer time immobile at the hotplate, suggesting an analgesic despair-like behavior. Additionally, chemogenetic activation of POMC neurons in mice mimicked the effect of restraint-induced stress in mice; also taking longer to escape from the hotplate. These results suggest that $POMC^{ARC}$ are involved in descending pain pathways in response[26] to restraint, promoting despair-like behavior through analgesic signaling in the CNS.

Another 2020 study also used restraint-induced stress to study $POMC^{ARC}$ role in modulating analgesic despair-like behavior seen after restraint. They found that restraint or $POMC^{ARC}$ activation leads to anhedonia and despair as measured through behavior like decreased glucose preference, and less mobility during forced swim and tail suspension. Using in vitro electrophysiology, the authors found that $POMC^{ARC}$ signals an inhibitory tone towards the ventral tegmental area (VTA) after restraint-induced stress; suggesting a circuit through which CNS responds to restraint stress. Moreover, introduction of cyprodime, a MOR antagonist, prevents the inhibitory tone evoked by the POMC neurons; suggesting involvement of β-endorphin release from POMC neurons for

effect[24]. These results make a compelling case of despair response to stress being modulated by preventing the inhibitory tone evoked by the POMC neurons; suggesting involvement of $POMC^{ARC}$ β- endorphin in despair as a response to stress.

In summary, social isolation induces a negative affective state in pups that activates opioid-mediated CNS pain response. In adults, distress-induced analgesic responses are thought to involve MOR and hypothalamic β-endorphin. However, in rodent pups, the role of endogenous opioids in distress-induced vocalizations is not clear. Here, we test mu opioid involvement in isolation-induced vocalizations using MOR receptor and β-endorphin knockouts. We also test the relationship of $POMC^{ARC}$ to opioid modulation of the behavior as a way to explore the circuit through which β-endorphin mediates its effects. Our findings ultimately shed light into the rise and adaptation of mammalian vocal behavior as well as requisites for healthy neural development.

3.3 Results

3.3.1 Activation of $POMC^{ARC}$ lowers the emission of isolation-induced vocalizations

To test whether $POMC^{ARC}$ neurons modulate isolation-induced vocalizations, I characterized the emission of vocalizations in mouse pups using gain- and loss-of-function of $POMC^{ARC}$ neurons. Importantly, mice vocalize above the human hearing range, emitting ultrasonic vocalizations (USVs). I quantified the emission of USV in ten days old mice (P10) during a prolonged period of separation (70 minutes). As a gain-of-function tool, I used Designer Receptors Exclusively Activated by Designer Drugs (Gq DREADD) to activate $POMC^{ARC}$ neurons. As a loss-of-function tool, I used the expression of the diphtheria toxin receptor to ablate $POMC^{ARC}$ neurons (**Figure 3.3.1**).

To analyze results, we use 2way-ANOVA, comparing effects of activation with control pups (Genotype) and the effect of USV emission across 70-minute isolation (Time).

I found that activation of $POMC^{ARC}$ neurons decreases the emission of USVs compared to littermate control pups (with no activation) (Control: 477.2 ± 90.4 USVs, N = 14; Activation: 258.0 ± 29.8 USVs, N = 8, *P = 0.02*; 2way-ANOVA; **Figure 3.3.2A**). Conversely, ablation of $POMC^{ARC}$ neurons increases the emission of USVs compared to controls (Control: 351.7 ± 32.8 USVs, N = 14; Ablation: 732.7 ± 56.3 USVs, N = 8; *P = 0.001*; 2way-ANOVA; **Figure 3.3.2B**). These results suggest that $POMC^{ARC}$ neurons modulate the emission of USVs during isolation in mouse pups.

Figure 0

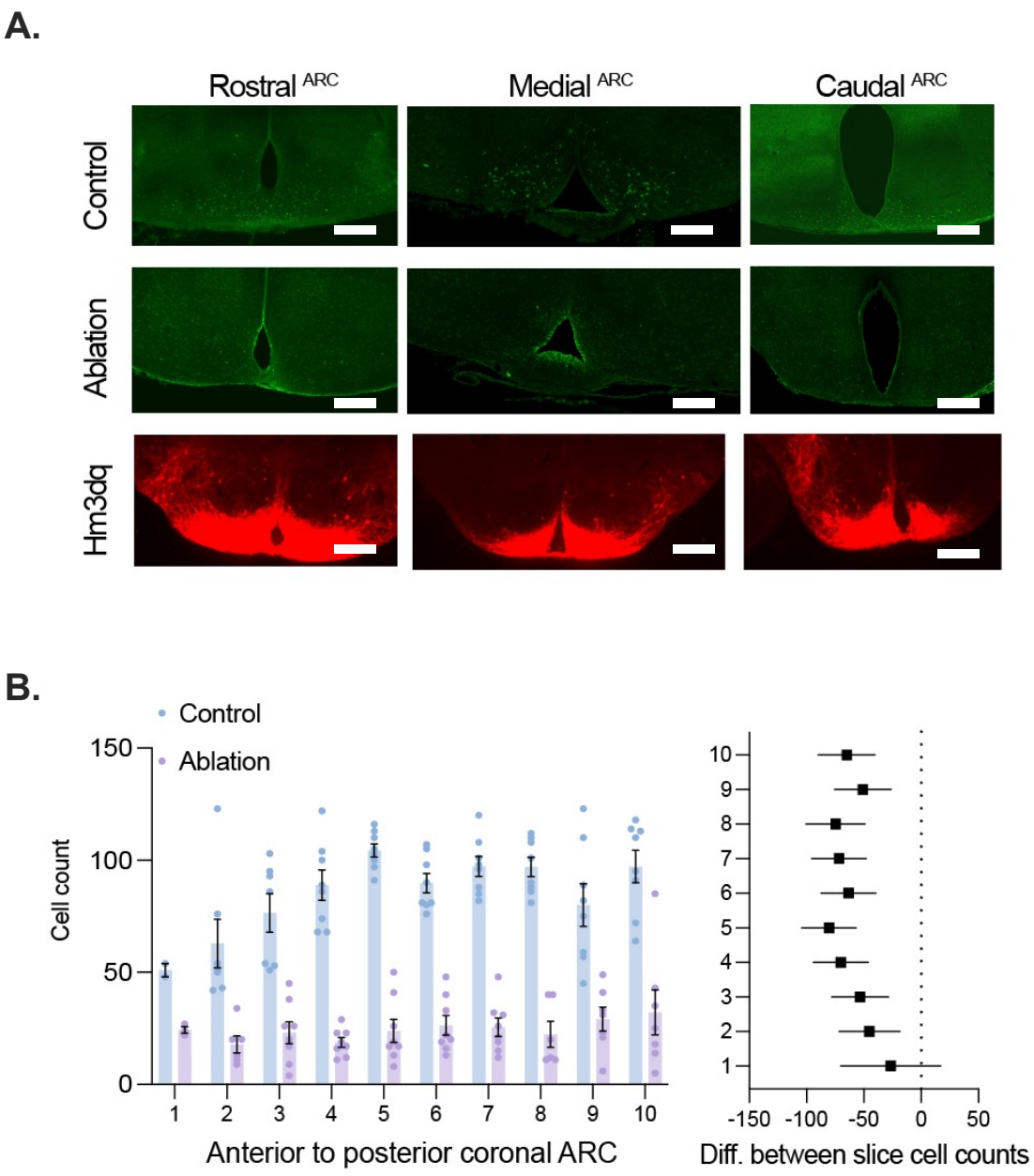

Figure 3.3.1. *<u>POMC^{ARC} neural ablation and activation viral infection.</u> (A) Confocal (20x) images of Hypothalamus ARC coronal sections. First two rows show GFP staining of POMC neurons after ablation in comparison to controls. Last row shows sections with*

DREADD infection. White scale on each image represents 50 microns. (B) Total POMC neurons counted across arcuate slides (70 microns, 10 slides for each).

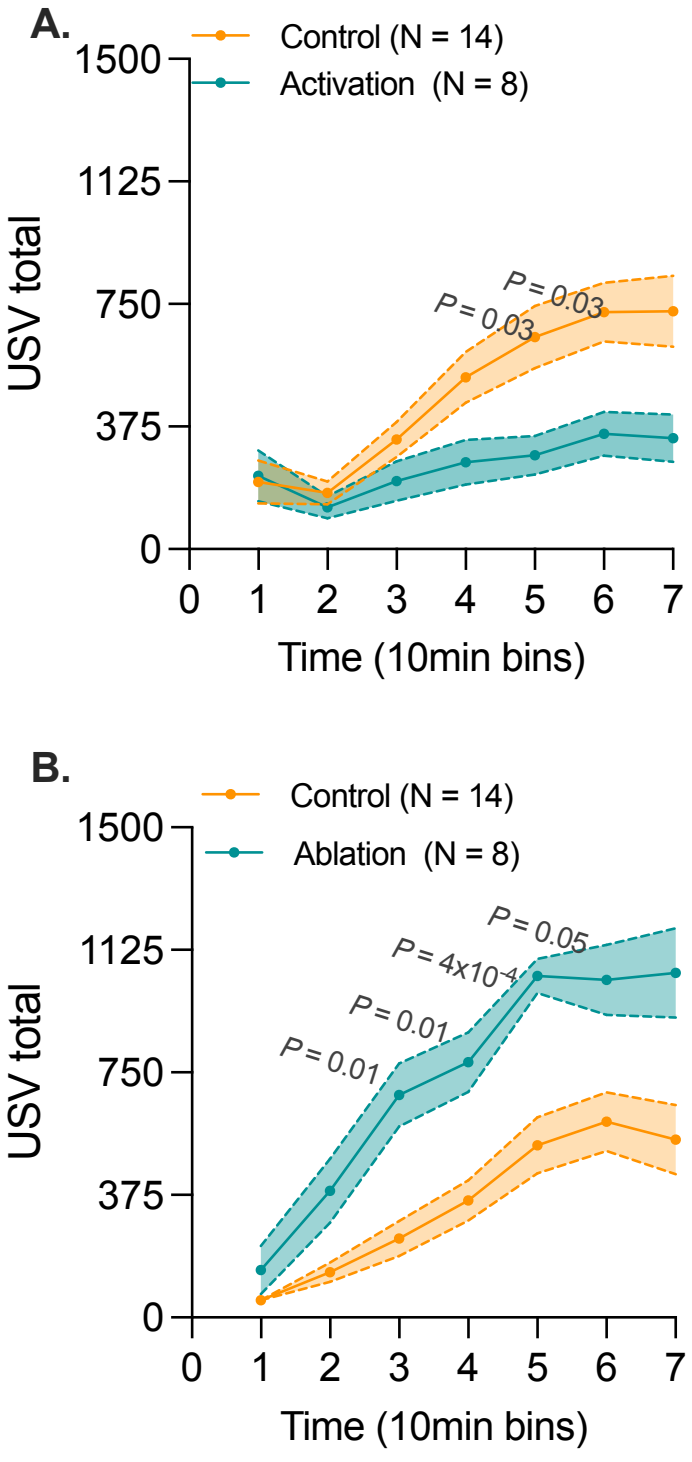

Figure 3.3.2. *<u>USV emission after POMC^{ARC} activation</u>. Pup vocalization across 70 minutes in 10-minute bins (baseline USV in first 10 minutes). Connected dot represent group average vocalization at each time mark. Shadowing over the dots represent standard error of mean. (A) POMC^{ARC} activation results.* (Genotype: $F_{1, 16}$ = 33.29, P = 3 x 10^{-5}; time: $F_{2, 41}$ = 19.23, P < 2 x 10^{-7}; genotype x age: $F_{6, 96}$ = 2.05, P = 2 x 10^{-6}; 2way-ANOVA) *(B) POMC^{ARC} ablation* (Genotype: $F_{1, 14}$ = 32.7, P = 3 x 10^{-12}; time: $F_{2, 35}$ = 50.6, P = 5 x 10^{-12}; genotype x age: $F_{6, 84}$ = 7.95, P = 8 x 10^{-7}; 2way-ANOVA).

3.3.2 <u>Activation of POMC^{ARC} changes vocal repertoire repetition and variability</u>

Next, I compared the vocal repertoire of pups upon activation of POMC^{ARC}. POMC^{ARC} increases the emission of 'short' USVs (Control: 0.3 ± 0.03 USVs, N = 14; Activation: 0.4 ± 0.06 USVs, N = 8; P = 0.003; Sidak's; **Figure 3.3.3A**) and suppress 'downward frequency modulation' (Control: 0.35 ± 0.02 USVs, N = 14; Activation: 0.2 ± 0.04 USVs, N = 8; P = 0.001; Sidak's; **Figure 3.3.3A**) and 'step-up' (Control: 0.15 ± 0.02 USVs, N = 14; Activation: 0.07 ± 0.02 USVs, N = 8; P = 0.001; Sidak's; **Figure 3.3.3A**). Conversely, ablation of POMC^{ARC} diminishes USVs of the class 'short' (Control: 0.35 ± 0.03 USVs, N = 14; Ablation: 0.27 ± 0.03 USVs, N = 8; P = 4 x 10^{-4}; Sidak's; **Figure 3.3.3B**).

A.

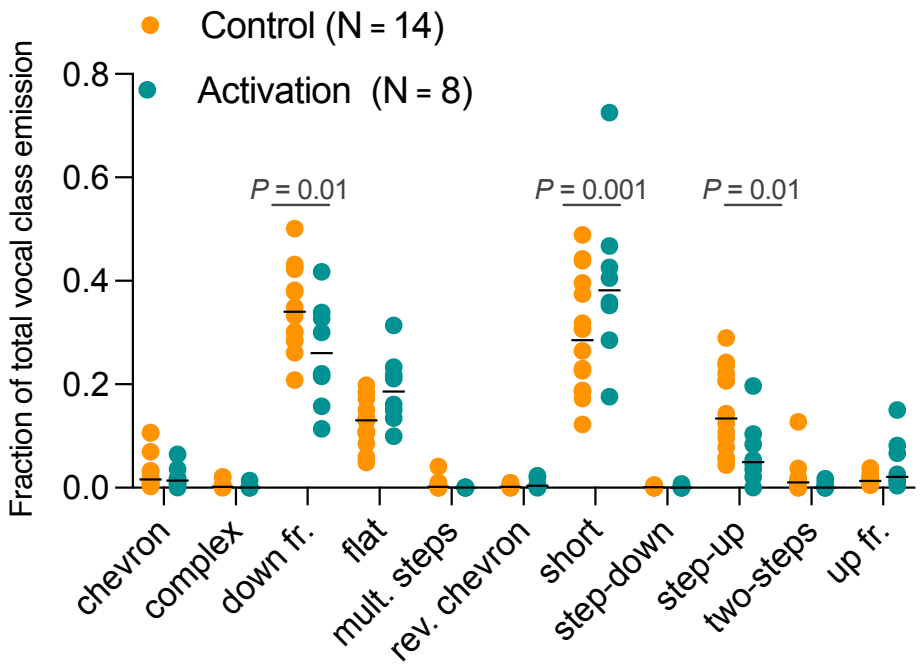
Control (N = 14)
Activation (N = 8)
Fraction of total vocal class emission
0.8
0.6
0.4
0.2
0.0
P = 0.01
P = 0.001
P = 0.01
chevron
complex
down fr.
flat
mult. steps
rev. chevron
short
step-down
step-up
two-steps
up fr.

B.

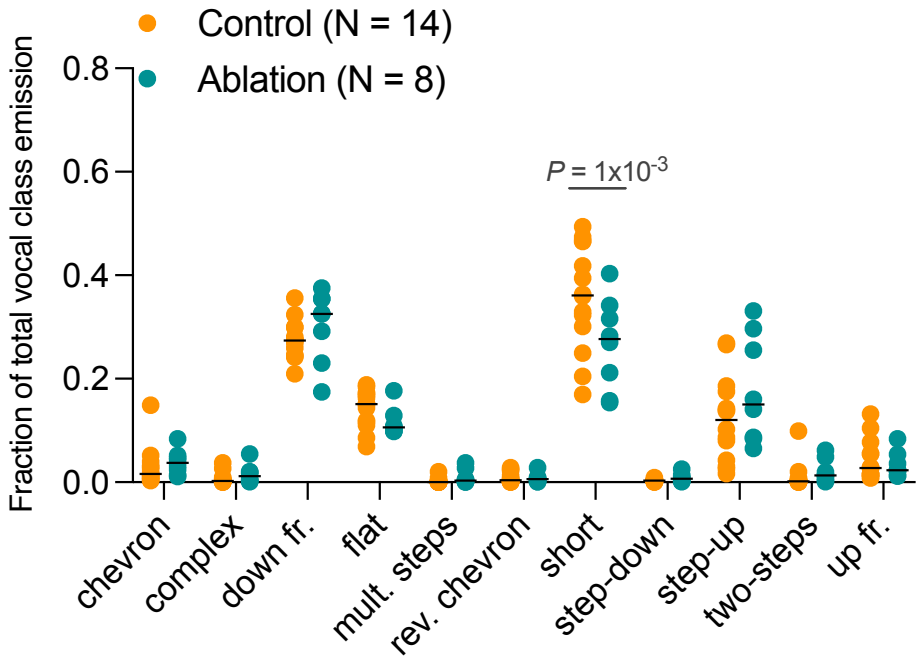
Control (N = 14)
Ablation (N = 8)
Fraction of total vocal class emission
0.8
0.6
0.4
0.2
0.0
P = 1x10-3
chevron
complex
down fr.
flat
mult. steps
rev. chevron
short
step-down
step-up
two-steps
up fr.

Figure 3.3.3. *<u>POMC^{ARC} activation changes vocal repertoire composition</u>. X axis represents each of the eleven syllable types. Distribution of syllable types in P10 pups during 60 minutes of isolation—control in orange and POMC activation in green. Data are showed as fraction of the total number of USVs; P values are found above from Sidak post-hoc analysis. (A) Activation vocal repertoire* (Genotype: *not significant*; class: $F_{10, 220} = 98.4$, $P = 5 \times 10^{-6}$; genotype x class: $F_{10, 220} = 4.6$, $P = 1 \times 10^{-15}$; 2way-ANOVA). (B) Ablation vocal repertoire (Genotype: *not significant*; class: $F_{10, 154} = 86.9$, $P = 1 \times 10^{-15}$; genotype x class: $F_{10, 154} = 2.4$, $P = 0.01$; 2way-ANOVA).

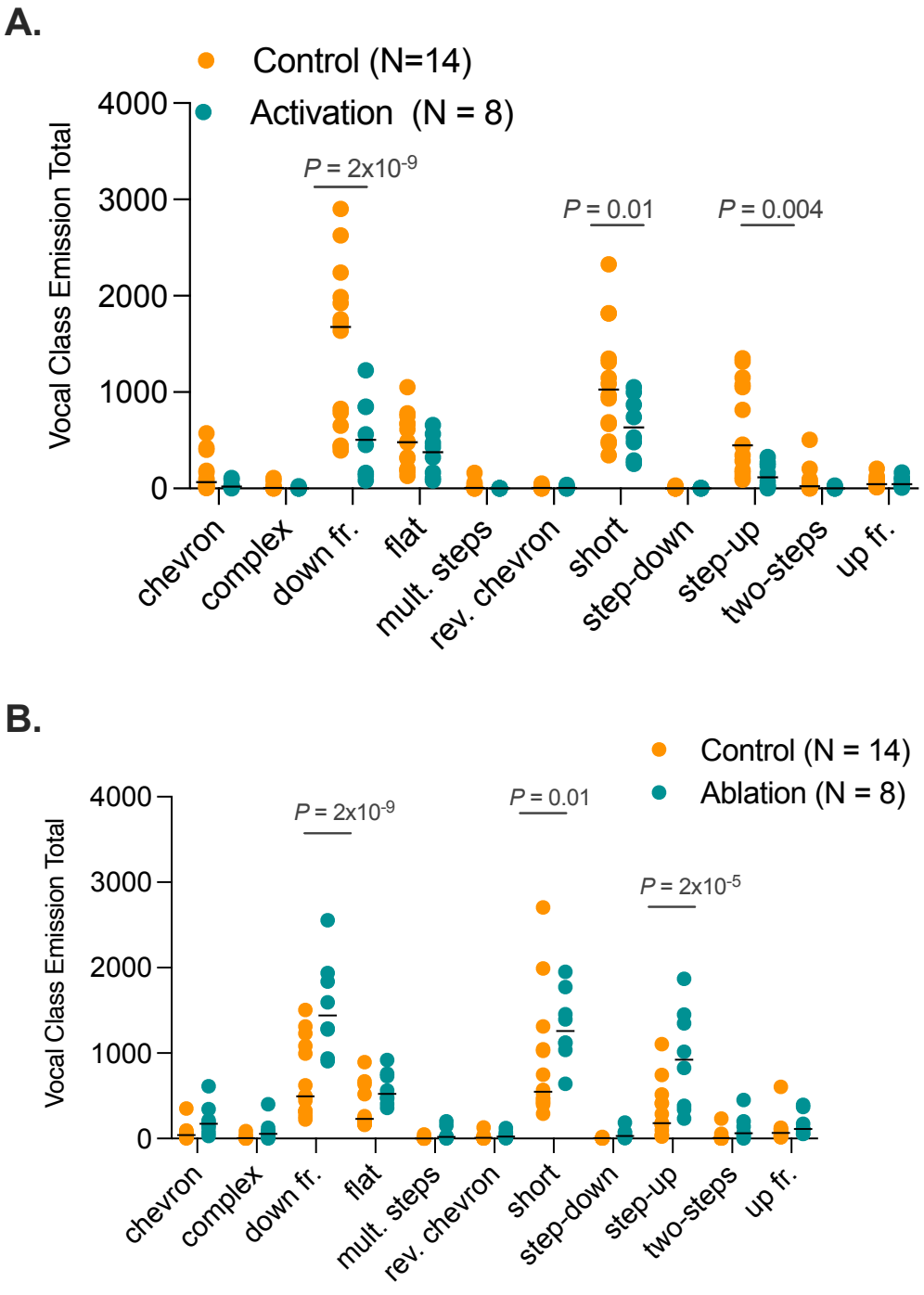

Figure 3.3.4 *POMC^{ARC} activation changes vocal class totals. X axis represents each of the eleven syllable types. Total count of USVs from each syllable type in P10 pups. Data*

are showed as fraction of the total number of USVs; P values are found above from Sidak post-hoc analysis. (A) Activation vocal repertoire (Genotype: $F_{1, 220}$ = 24, P = 2 x 10^{-6}; Class: $F_{10, 220}$ = 28.5, P < 1 x 10^{-16}; Interaction: $F_{10, 220}$ = 4.7, P = 4 x 10^{-6}; 2way-ANOVA*). (B) Ablation vocal repertoire (Genotype: $F_{1, 220}$ = 40, P = 2 x 10^{-9}; class: $F_{10, 220}$ = 44, P < 1 x 10^{-16}; genotype x class: $F_{10, 220}$ = 4.7, P = 5 x 10^{-5};* 2way-ANOVA*).*

3.3.3 $POMC^{ARC}$ neurons require μ opioid receptors to change USV rate

I next tested the extent to which the effects of $POMC^{ARC}$ neurons on the emission of USVs in pups depends on mu-opioid receptor signaling. Hence, I activated $POMC^{ARC}$ neurons in pups that were knockouts for μ receptors (*Orpm1-KO)*. Litters for this experiment were obtained by breeding heterozygous *$Orpm1^{Tm1/Kff}$* dams with heterozygous males for both *$Orpm1^{Tm1/Kff}$* and $POMC^{Cre}$. Our experimental group includes Cre+ (activation) and Cre- pups of wild-type (Orpm1-WT) and Orpm1-KO background.

Orpm1-WT pups show similar USV rates to our previous activation experiment (Orpm1-WT: 310.7 ± 49.7 USVs, N = 18; Activation: 130.9 ± 23.4 USVs, N = 14; *P* = 0.001; 2way-ANOVA; **Figure 3.3.5A**). In contrast, activation of $POMC^{ARC}$ neurons in Orpm1-KO pups did not change USV rate compared to Orpm1-KO pups (Orpm1-KO: 329.6 ± 57.5 USVs, N = 9; Activation: 361 ± 50.4 USVs, N = 8; *P* = 0.74; 2way-ANOVA; **Figure 3.3.5B**).

We also analyzed rates using 3way-ANOVA to measure the contribution of genotype, time, and activation as the source of variation. We found that time ($F_{6,336}$ = 12.1; *P* = 3 X 10^{-12}; 3way-ANOVA) genotype ($F_{1,336}$ = 23.6; *P* = 2 X 10^{-6}; 3way-ANOVA), and activation ($F_{1,336}$ = 8.4; *P* = 0.004; 3way-ANOVA) significantly contribute to differences in

phenotype. Additionally, interaction between genotype and activation was significant ($F_{1,336}$ = *0.38; P* = 5 X 10^{-5}; 3way-ANOVA) while interaction between time with genotype or activation, or the three together was not significant.

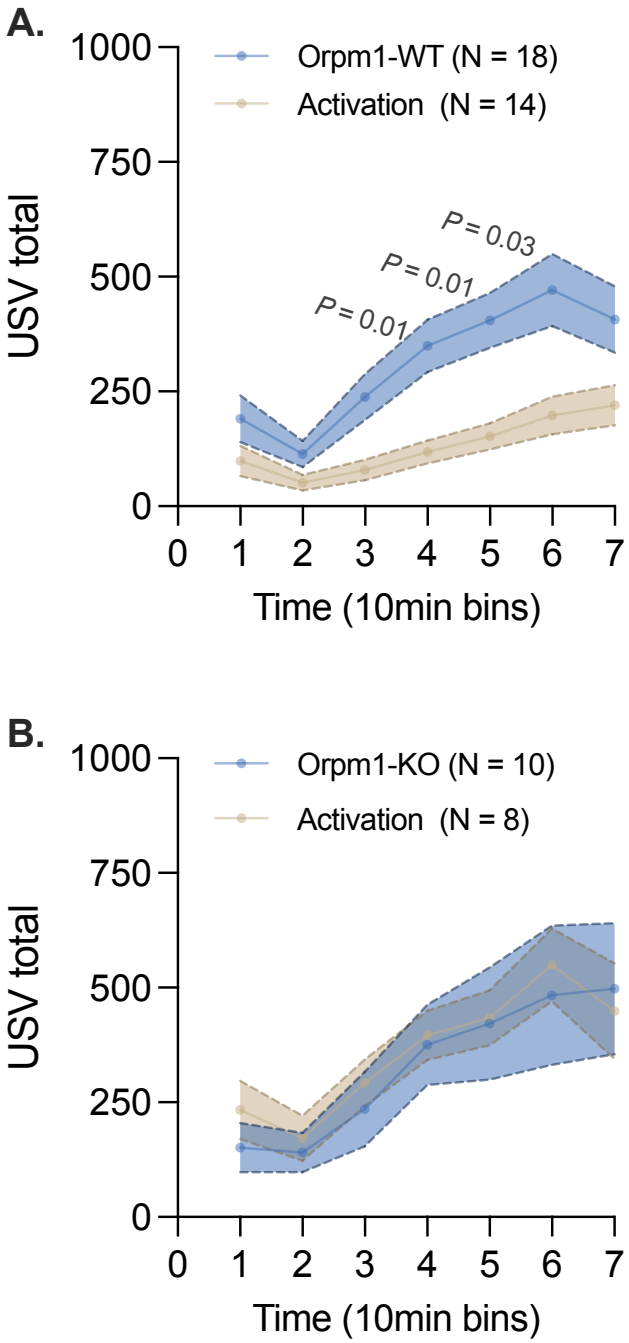

Figure 3.3.5. *USV emission drops via POMC^{ARC} activation of MOR. Pup vocalization across 70 minutes in 10-minute bins (baseline USV in first 10 minutes). (A.) Orpm1-WT (*Genotype: $F_{1, 89}$ = 45.9, P = 2 x 10^{-10}; time: $F_{6, 189}$ = 11.2, P = 1 x 10^{-10}; genotype x age: $F_{6, 189}$ = 2.2, P = 0.04; 2way-ANOVA). (B.) Orpm1-KO (No significant differences found).

3.3.3 Activation of POMC^{ARC} require μ opioid receptors for changes in USV classes

Orpm1-WT activation also displayed similar differences in vocal repertoire as before; activation promoted more short vocal emission (Orpm1-WT: 0.28 ± 0.03 USVs, N = 18; Activation: 0.38 ± 0.03 USVs, N = 16; P = 6 x 10^{-5}; Sidak's; **Figure 3.3.5A**) less down-frequency (Orpm1-WT: 0.4 ± 0.03 USVs, N = 18; Activation: 0.34 ± 0.02 USVs, N = 16; P = 0.05; Sidak's; **Figure 3.3.5A**), and less step-up calls (Orpm1-WT: 0.15 ± 0.03 USVs, N = 18; Activation: 0.09 ± 0.02 USVs, N = 16; P = 0.04; Sidak's; **Figure 3.3.5A**). We also found that POMC activation in Orpm1-KO pups leads to less short calls than controls (Orpm1-KO: 0.36 ± 0.04 USVs, N = 9; activation: 0.25 ± 0.01 USVs, N = 8; P = 0.002; Sidak's; **Figure 3.3.5B**).

Additionally, total vocal class emission remains consistent for Orpm1-WT with POMC activation leading to less down fr., short, and step-up calls. Moreover, vocal class use did not differ with POMC^{ARC} activation without MOR (**Figure 3.3.6**). 3way-ANOVA analysis of vocal class total reports a three-way interaction between vocal class, genotype, and activation ($F_{10,480}$ = 3; P = 0.001). These results suggest that MOR downstream POMC^{ARC} inhibits pup vocalization but MOR downstream does not affect strain selection.

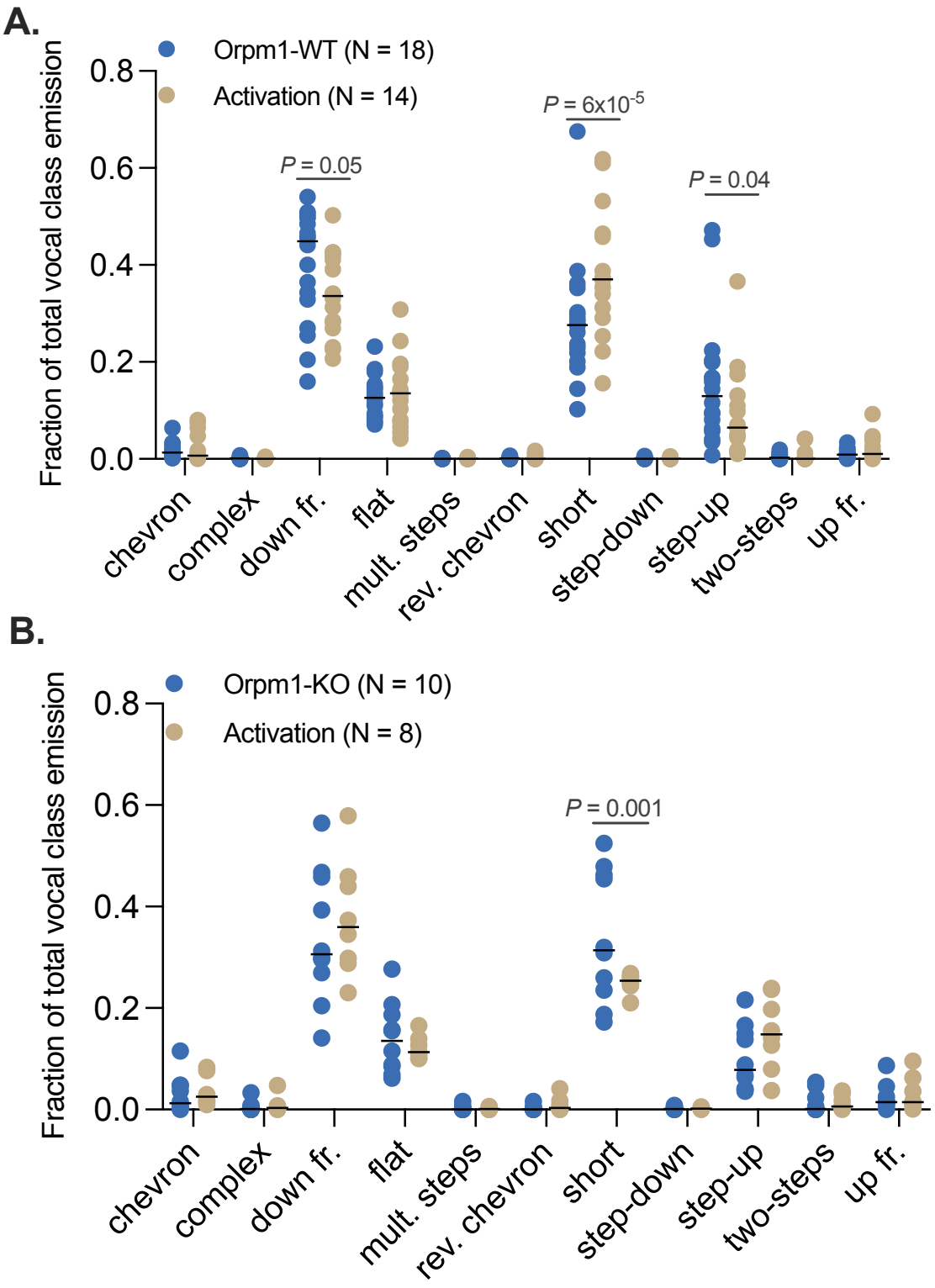
A.
Orpm1-WT (N = 18)
Activation (N = 14)
Fraction of total vocal class emission
0.8
0.6
0.4
0.2
0.0
P = 0.05
P = 6x10-5
P = 0.04
chevron
complex
down fr.
flat
mult. steps
rev. chevron
short
step-down
step-up
two-steps
up fr.
B.
Orpm1-KO (N = 10)
Activation (N = 8)
Fraction of total vocal class emission
0.8
0.6
0.4
0.2
0.0
P = 0.001
chevron
complex
down fr.
flat
mult. steps
rev. chevron
short
step-down
step-up
two-steps
up fr.

Figure 3.3.6*. POMC^{ARC} changes vocal repertoire through MOR. Distribution of syllable types in P10 pups during 60 minutes of isolation. P values are found above from Sidak post-hoc analysis. (A) Wildtype background activation (*Genotype: *not significant*; Class: $F_{10, 352}$ = 162, $P < 1 \times 10^{-15}$; genotype x age: $F_{10, 352}$ = 3.8, $P = 1 \times 10^{-4}$; 2way-ANOVA). *(B) Orpm1-KO activation (Genotype: not significant; Class: $F_{10, 176} = 90.8$; $P < 1 \times 10^{-16}$; genotype x class: Not significant;* 2way-ANOVA*).*

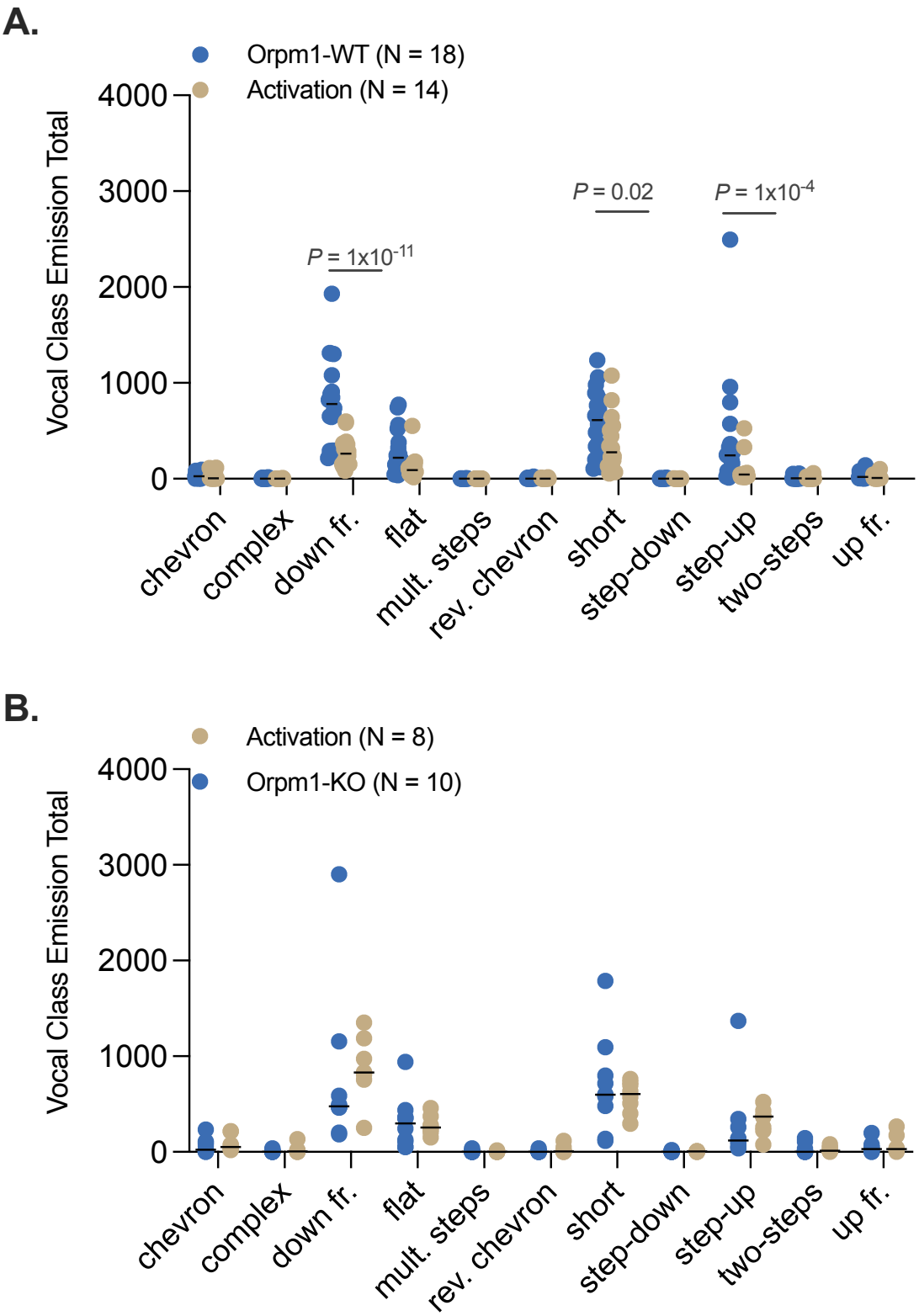
A.
Orpm1-WT (N = 18)
Activation (N = 14)
Vocal Class Emission Total
4000
3000
2000
1000
0
P = 1x10-11
P = 0.02
P = 1x10-4
chevron
complex
down fr.
flat
mult. steps
rev. chevron
short
step-down
step-up
two-steps
up fr.
B.
Activation (N = 8)
Orpm1-KO (N = 10)
Vocal Class Emission Total
4000
3000
2000
1000
0
chevron
complex
down fr.
flat
mult. steps
rev. chevron
short
step-down
step-up
two-steps
up fr.

Figure 3.3.7. *<u>POMC^{ARC} activation affects vocal class totals</u>. X axis represents each of the eleven syllable types. P values are found above from Sidak post-hoc analysis. (A) Activation vocal repertoire (Genotype: $F_{1, 352} = 29.5$, $P = 1 \times 10^{-7}$; Class: $F_{10, 352} = 36.8$, $P < 1 \times 10^{-16}$; Interaction: $F_{10, 352} = 6.2$, $P = 1 \times 10^{-8}$;* 2way-ANOVA*). (B) Orpm1-KO activation vocal repertoire (Genotype: not significant; Class: $F_{10, 176} = 21.5$, $P < 1 \times 10^{-16}$; Interaction: not significant;* 2way-ANOVA*).*

<u>3.3.4 β-endorphin drops vocal rate and promotes "short" call USVs</u>

Next, I tested the significance of β-endorphin on the emission of distress vocalizations. I used mice deficient for the production of β-endorphin generated by intercrossing heterozygous β-endorphin knockouts (*Pomc tm1Low)* mice. From the same litter, I analyzed isolation-induced USVs from mutant (βE-KO) and wild-type pups (Control) at P10. β-Endorphin deficient mice showed higher rates of USVs in comparison to control (Control: 307.3 ± 24.6 USVs, N = 19; βE-KO: 582.7 ± 70.7 N = 16 USVs; $P = 1 \times 10^{-5}$; 2way-ANOVA; **Figure 3.3.8A**). Additionally, β-endorphin knockout pups use fewer short calls than controls (Control: 0.43 ± 0.03 USVs, N = 19; βE-KO: 0.34 ± 0.03, n = 24; P = 0.01; Sidak's; **Figure 3.3.9B**).

Similar to the POMC^{ARC} ablation effects, total count of vocal classes emitted show that βE-KO used more down fr. (Control: 575 ± 81 USVs, N = 19; βE-KO: 1233 ± 165, N = 16; $P = 2 \times 10^{-19}$; Sidak's; **Figure 3.3.9B**), short (Control: 951 ± 155 USVs, N = 19; βE-KO: 1379 ± 197, N = 16; $P = 4 \times 10^{-4}$; Sidak's; **Figure 3.3.9B**), and step-up total emissions in comparison to controls (Control: 228 ± 49 USVs, N = 19; βE-KO: 604 ± 127, N = 16; $P = 6 \times 10^{-9}$; Sidak's; **Figure 3.3.9B**).

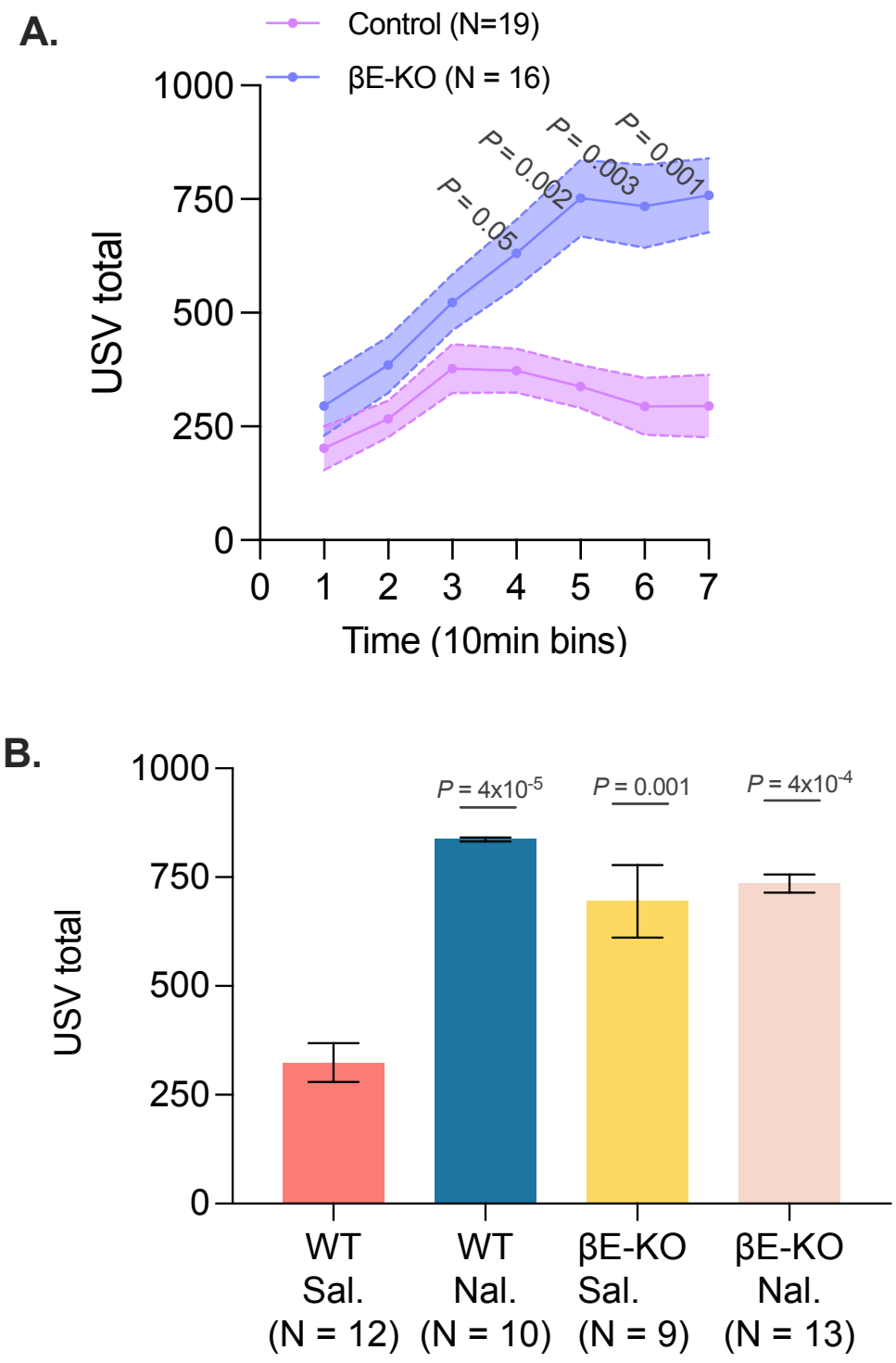
A.
Control (N=19)
βE-KO (N = 16)
1000
750
500
250
0
USV total
P = 0.05
P = 0.002
P = 0.003
P = 0.001
0 1 2 3 4 5 6 7
Time (10min bins)
B.
1000
750
500
250
0
USV total
P = 4x10-5
P = 0.001
P = 4x10-4
WT Sal. (N = 12)
WT Nal. (N = 10)
βE-KO Sal. (N = 9)
βE-KO Nal. (N = 13)

Figure 3.3.8.

(A)USV emission of P10 β-endorphin knockout pups maintains a higher USV rate. Pup vocalization across 70 minutes in 10-minute bins. P values are found above from Sidak post-hoc analysis. (Genotype: $F_{1, 33}$ = 18.9, P = 1 x 10^{-4}; time: $F_{2, 67}$ = 10.7, P = 1 x 10^{-4}; genotype x age: $F_{6, 198}$ = 5.4, P = 1 x 10^{-5}; 2way-ANOVA).

(B) *Opioid antagonist naloxone reverses pup USV emission rate* P10. *Graph shows rate of knockout and control pups after saline or naloxone injection. We recorded 30 min before (baseline) and after injection. Only last 30 minutes USV plotted. P values are found above from Sidak post-hoc analysis of each group with Orpm1-WT activation.* (Genotype: *not significant*; Time: $F_{3, 134}$ = 24.3, P < 1 x 10^{-13}; Treatment (saline or naloxone): $F_{1, 40}$ = 8.3, P = 0.01; Interaction (time x genotype x treatment: $F_{5, 200}$ = 3.7, P = 0.01=03; 3way-ANOVA).

Treatment of wildtype pups with the opioid receptor antagonist naloxone increases the emission of USVs in comparison to saline-injected controls (Saline: 323.3 ± 47 USV/10min, N = 12; Naloxone: 837 ± 4.6 USV/10min, N = 10; P = 0.002; Sidak's; **Figure 3.3.8B**). Importantly, treatment of β-endorphin deficient pups with naloxone did not affect the emission of USVs (Saline: 647 ± 83 USV/10min, N = 9; Naloxone: 736 ± 21 USV/10min, N = 13; P = 0.78; Sidak's; **Figure 3.3.8B**).

I also used 3way-ANOVA to identify contributing factors to phenotypic differences. While genotype and time were not significant, treatment (naloxone vs saline) contributes significantly to variation seen between groups ($F_{1,40}$ = 7.5; P = 0.01; 3way-ANOVA). Moreover, treatment significantly interacts with time ($F_{3,120}$ = 5.5; P = 0.002; 3way-ANOVA) and genotype ($F_{1,40}$ = 5.4; P = 0.03; 3way-ANOVA) but time interaction with genotype nor the three together show significant contribution. Our results suggest that endogenous β-endorphin influence USV rate during isolation.

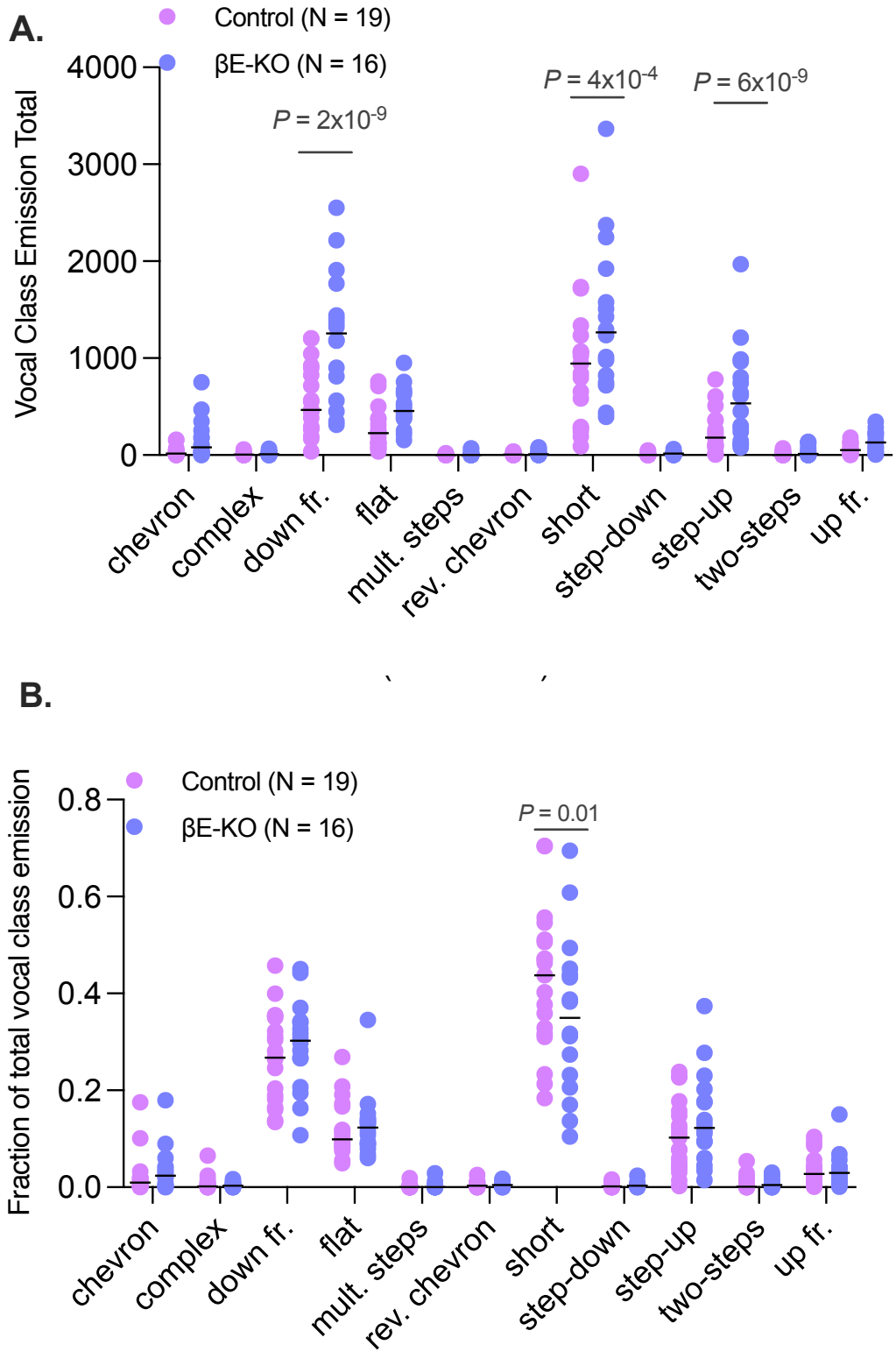
A.
Control (N = 19)
βE-KO (N = 16)
Vocal Class Emission Total
4000
3000
2000
1000
0
P = 2x10-9
P = 4x10-4
P = 6x10-9
chevron
complex
down fr.
flat
mult. steps
rev. chevron
short
step-down
step-up
two-steps
up fr.
B.
Control (N = 19)
βE-KO (N = 16)
Fraction of total vocal class emission
0.8
0.6
0.4
0.2
0.0
P = 0.01
chevron
complex
down fr.
flat
mult. steps
rev. chevron
short
step-down
step-up
two-steps
up fr.

Figure 3.3.9.*USV class repertoire totals of P10 β-endorphin knockout X axis represents each of the eleven syllable types. Distribution of syllable types in P10 pups during 60 minutes of isolation. (A)Data are showed as total number of USVs; (B) Data showed as fraction from total USV emission. P values are found above from Sidak post-hoc analysis.* (Genotype: *not significant;* Class: $F_{10, 638} = 242$, $P < 1 \times 10^{-15}$; genotype x age: *not significant*; 2way-ANOVA)

3.4 Discussion

Social isolation induces a negative affective state in pups that activates opioid-mediated CNS pain response[6,7]. In adults, distress-induced analgesic responses are thought to involve MOR and hypothalamic β-endorphin[1,27]. In rodent pups, the role of endogenous opioids in distress-induced vocalizations is not clear since labs report contradicting results about opioid antagonist reversal of opioid effects on infant vocalization[16].

Here, we tested the involvement of the opioidergic system in isolation-induced vocalizations using MOR receptor and β-endorphin knockouts mice in addition to pharmacological blockade of opioid receptor signaling with naloxone. Finally, we also tested the extent to which $POMC^{ARC}$ neurons, which produce β-endorphin in the brain, affect isolation-induced vocalizations in a MOR-dependent manner.

The emission of isolation-induced by mouse pups drops with the activation of $POMC^{ARC}$ neurons and increases with the ablation of these neurons. Strikingly, in MOR knockout mice, activation of $POMC^{ARC}$ neurons does not affect USVs, suggesting that β-endorphin released by $POMC^{ARC}$ neurons signals via MOR receptor to affect distress vocalizations in pups. To further test this assumption, we characterized the vocal behavior of β-

endorphin deficient mice, showing a higher rate of USVs, a phenotype similar to pups injected with the opioid antagonist, naloxone. However, naloxone injection in β-endorphin deficient pups did not increase the emission of USVs, further suggesting that the modulation of distress vocalizations in pups is mediated by β-endorphin signaling. Put together, our results demonstrate how different components of the endogenous opioidergic system affect infant vocal behavior.

In parallel to changes in vocal rate, there were consistent changes in the emission of USVs of the classes 'down-frequency modulation', 'short', and 'step-up'. Manipulations that increased the emission of USVs--$POMC^{ARC}$ neuron ablation and β-endorphin deficient mice—decreased the emission of 'short' calls, while manipulations that decreased the emission of USVs—activation of $POMC^{ARC}$ neurons—increased the emission of 'short' calls.

These changes in vocal rate and in vocal repertoire do not seem to be caused by physiological factors like weight or temperature (**Figure 3.7.1-2**). At postnatal day 10, pups can maintain a constant baseline temperature for 90 minutes of isolation. Additionally, at this age and during this period of isolation, corticosterone levels do not increase[28], in line with the lack of recruitment of the hypothalamus-pituitary axis (HPA) during separation distress in infants. One interpretation for these results is that conditions of higher 'psychological' distress—and, therefore, of higher arousal—leads to the emission of more USVs that are also more complex.

Hypothalamic POMC neuron contribution to infant distress USVs shares some functional similarities to POMC neuron's role in "stress-induced analgesia" (SIA). SIA is evoked through the CNS in response to mild and acute stress as a way to cope with ongoing

negative state[2]. As elaborated in the first chapter, β-Endorphin promotes SIA despair behavior to cope with social and other forms of mild stress[29]. It would be interesting to further explore similarities between adult SIA and infant despair-induced USV reduction. Especially, whether they are part of the same or overlapping CNS response pathway.

Study of infant pups is in part limited by the narrow set of experimental manipulations that can be applied successfully. To advance the study of the role of $POMC^{ARC}$ neurons and opioid signaling on pup behavior, future studies should involve *in vivo* measurement of $POMC^{ARC}$ neuron activity as well as in vivo measurements of β-endorphin dynamics. Given the importance of understanding the development of normal attachment and social behaviors, the studies reported here provide new insights on the importance of hypothalamic neurons in the regulation of infant cry. These studies provide an entry point to study upstream and downstream neuronal circuits that are involved in infant behavior.

3.5 Methods

3.5.1. Experimental models and subject details

All preweaning mice used in the experiments were 9 to 10 days old from both sexes. Litters for POMC neuron activation and ablation were generated by breeding $POMC^{Cre}$ males (#005965, Jackson laboratory) with C57BL/6J (Jax #000664) females. Litters for POMC neuron activation with Orpm1 knockout background were generated by first breeding $POMC^{Cre}$ males with Orpm1 knockout females (#007559, Jackson laboratory). Orpm1 heterozygous males that were Cre+ were bred with heterozygous Orpm1 heterozygous females. Litters for β-endorphin knockout (#003191, Jackson laboratory) were generated by breeding heterozygous mutants. Separate litters were used in naloxone experiments. Dams used were 2 to 6 months old. All mice were kept in temperature- and humidity-controlled rooms, in a 12/12 hr. light/dark cycle, with lights on from 7:00 AM–7:00 PM. Studies took place during the light cycle. Food (Teklad 2018S, Envigo) and water were provided ad libitum. All procedures were approved by IACUC (Yale University).

Experiment	Litters	Experimental N	Control N
POMC neuron activation	7	8	14
POMC neuron ablation	6	8	14
β-endorphin knockout	15	15	18
Saline	15	9	12
Naloxone		14	9
Orpm1 KO control	20	16	18
Orpm1 KO		8	10

3.5.2. Viral injections at p0

For activation of POMC neurons, we used AAV8-hSyn-DIO-hM3D(Gq)-mCherry (#44361-AAV8, Addgene); for neural ablation we used AAV1-Flex-taCasp3-TEVP (#45580, Addgene). Pups are removed from the home cage and placed in an aluminum

vessel surrounded by ice for 10 minutes to induce hypothermia anesthesia. They are then placed in a stereotaxic frame with ear bars designed for neonates. A stereotaxic manipulator is used to position the syringe. Viral vectors (AAVs) are injected bilaterally at a volume of 0.3 µl per side using the following coordinates from lambda: AP = +.98 ML, lateral = -0.3mm, DV = -4.1.

3.5.3. Immunohistochemistry

Mice are deeply anesthetized and perfused with freshly prepared fixative (paraformaldehyde 4%, in PBS 1x [pH = 7.4]). Brains are post-fixed overnight in fixative. Tissue is sectioned at 100 µm in coronal orientation, allowing for efficient visualization of fibers extending through the brain without overlap. These sections are washed several times in PBS 1x (pH = 7.4) and pre-incubated with Triton X-100 (0.3% in PBS 1x) for 30 min. Sections are then incubated in a blocking solution (Triton 0.3%, Donkey Serum 10%, Glycine 0.3M in PBS 1x) for one hour. To confirm virus expression, brains were incubated with rabbit polyclonal anti-mcherry (1:1000; sc-52, Santa Cruz Biotechnologies) or chicken monoclonal anti-EGFP (1:1000, ab13970, abcam) for 16 hrs. After, sections are washed in 0.3% Triton in PBS, incubated with secondary fluorescent Alexa antibodies (1:500) for 4 hours, and washed once more with PBS.

3.5.4. Isolation-induced vocalization behavior protocol

Pups from the same litter were placed individually in a soundproof chamber containing fresh bedding material[28,30]. An UltraSoundGate Condenser Microphone CM 16 (Avisoft Bioacoustics, Berlin, Germany) was placed 10 cm above the recording chamber and connected to the UltraSoundGate 416 USGH device to record ultrasonic vocalizations.

The recording sessions lasted 70 minutes. Four to eight chambers were recorded simultaneously. After testing, mice were placed back in their home cage with the dam.

In neuron activation experiments, pups were recorded in isolation for 10 minutes (baseline) before being intraperitoneal injection with DREADD ligand, clozapine-N-oxide (CNO 1 mg/kg in saline). Once injected, pups were placed back in isolation for another hour recording. For naloxone experiments, pups were recorded for 30-minute baseline then injected with naloxone (5 mg/kg in saline) or saline (control); after, pups are placed back for another 30-minute recording.

3.5.5. Vocalization analysis

USVs will be automatically extracted from the audio recordings by custom-built software using spectral analysis through image processing. The spectrograms are converted to grayscale images and the vocalizations are segmented on the spectrogram through a sequence of image processing techniques. The segmented vocalization candidates are then analyzed by a local median filtering to eliminate segmentation noise based on the contrast between a vocalization candidate and its background. Next, all the vocalizations are classified in 11 distinct call types (Grimsley, 2011) by a Convolutional Neural Network, which had the AlexNet architecture as starting point. The network was trained for USV classification with over 14,000 samples of real vocalizations, which are then augmented in order to increase the variability of the samples, resulting in >57,000 samples. Each vocalization receives a label based on the most likely call type label attributed by the Convolutional Neural Network. The label of each USV is also available as a probability distribution function over all the call types.

3.5.6. Quantification and statistical analysis

Prism 8.0 or above was used to analyze data and plot figures. Shapiro-Wilk normality test was used to assess normal distribution of the data. To analyze differences in the use of harmonics, we used the non-parametric Mann-Whitney Test with Bonferroni correction to find statistically different effects. The data was analyzed using two-way ANOVA or mixed-effects analysis. For Orpm1 and Naloxone experiments, 3-wayANOVA was used. Sidak's multiple comparisons test was used to find post hoc differences among groups and to calculate the 95% confidence intervals to report effect size. In the text, values are provided as mean ± SEM. $P < 0.05$ was considered statistically significant and, when necessary and as described above, was corrected using Bonferroni's method. Statistical data are provided in text and in the figures.

3.5 References

1. Ferdousi M, Finn DP. Stress-induced modulation of pain: Role of the endogenous opioid system. *Prog Brain Res.* 2018;239:121-177.
2. Amit Z, Galina ZH. Stress-induced analgesia: adaptive pain suppression. *Physiol Rev.* 1986;66(4):1091-1120.
3. Herman BH, Panksepp J. Ascending endorphin inhibition of distress vocalization. *Science.* 1981;211(4486):1060-1062.
4. Butler RK, Rea K, Lang Y, Gavin AM, Finn DP. Endocannabinoid-mediated enhancement of fear-conditioned analgesia in rats: opioid receptor dependency and molecular correlates. *Pain.* 2008;140(3):491-500.
5. Butler RK, Finn DP. Stress-induced analgesia. *Prog Neurobiol.* 2009;88(3):184-202.
6. Panksepp J, Meeker R, Bean NJ. The neurochemical control of crying. *Pharmacol Biochem Behav.* 1980;12(3):437-443.
7. Panksepp J, Watt D. Why does depression hurt? Ancestral primary-process separation-distress (PANIC/GRIEF) and diminished brain reward (SEEKING) processes in the genesis of depressive affect. *Psychiatry.* 2011;74(1):5-13.
8. Newman JD. Neural circuits underlying crying and cry responding in mammals. *Behav Brain Res.* 2007;182(2):155-165.
9. Lingle S, Wyman MT, Kotrba R, Teichroeb LJ, Romanow CA. What makes a cry a cry? A review of infant distress vocalizations. *Current Zoology.* 2012;58(5):698-726.
10. Nelson EE, Panksepp J. Brain substrates of infant-mother attachment: contributions of opioids, oxytocin, and norepinephrine. *Neurosci Biobehav Rev.* 1998;22(3):437-452.

11. Lingle S, Riede T. Deer mothers are sensitive to infant distress vocalizations of diverse mammalian species. *Am Nat.* 2014;184(4):510-522.
12. Hofer MA, Shair HN, Brunelli SA. Ultrasonic vocalizations in rat and mouse pups. *Curr Protoc Neurosci.* 2002;Chapter 8:Unit 8 14.
13. Kehoe P, Blass EM. Behaviorally functional opioid systems in infant rats: II. Evidence for pharmacological, physiological, and psychological mediation of pain and stress. *Behav Neurosci.* 1986;100(5):624-630.
14. Panksepp J, Herman BH, Vilberg T, Bishop P, DeEskinazi FG. Endogenous opioids and social behavior. *Neurosci Biobehav Rev.* 1980;4(4):473-487.
15. Kalin NH, Shelton SE, Barksdale CM. Opiate modulation of separation-induced distress in non-human primates. *Brain Res.* 1988;440(2):285-292.
16. Carden SE, Hofer MA. Isolation-induced vocalization in Wistar rat pups is not increased by naltrexone. *Physiol Behav.* 1991;49(6):1279-1282.
17. Moles A, Kieffer BL, D'Amato FR. Deficit in attachment behavior in mice lacking the mu-opioid receptor gene. *Science.* 2004;304(5679):1983-1986.
18. Corder G, Castro DC, Bruchas MR, Scherrer G. Endogenous and Exogenous Opioids in Pain. *Annu Rev Neurosci.* 2018;41:453-473.
19. Froehlich JC. Opioid peptides. *Alcohol Health Res World.* 1997;21(2):132-136.
20. Watkins LR, Mayer DJ. Organization of endogenous opiate and nonopiate pain control systems. *Science.* 1982;216(4551):1185-1192.
21. Veening JG, Gerrits PO, Barendregt HP. Volume transmission of beta-endorphin via the cerebrospinal fluid; a review. *Fluids Barriers CNS.* 2012;9(1):16.
22. Joseph SA, Michael GJ. Efferent ACTH-IR opiocortin projections from nucleus tractus solitarius: a hypothalamic deafferentation study. *Peptides.* 1988;9(1):193-201.

23. Pilozzi A, Carro C, Huang X. Roles of beta-Endorphin in Stress, Behavior, Neuroinflammation, and Brain Energy Metabolism. *Int J Mol Sci.* 2020;22(1).
24. Lee EJ, Hanchate NK, Kondoh K, et al. A psychological stressor conveyed by appetite-linked neurons. *Sci Adv.* 2020;6(12):eaay5366.
25. Hennessy MB, Schreibeis AD, Schiml PA, Deak T. Maternal separation increases later immobility during forced swim in guinea pig pups: evidence for sensitization of a depressive-like state. *Dev Psychobiol.* 2017;59(1):128-132.
26. Qu N, He Y, Wang C, et al. A POMC-originated circuit regulates stress-induced hypophagia, depression, and anhedonia. *Mol Psychiatry.* 2020;25(5):1006-1021.
27. Seo YJ, Kwon MS, Choi SM, et al. Differential cross-tolerance development between single and repeated immobilization stress on the antinociceptive effect induced by beta-endorphin, 5-hydroxytryptamine, morphine, and WIN55,212-2 in the inflammatory mouse pain mode. *Arch Pharm Res.* 2011;34(2):269-280.
28. Zimmer MR, Fonseca AHO, Iyilikci O, Pra RD, Dietrich MO. Functional Ontogeny of Hypothalamic Agrp Neurons in Neonatal Mouse Behaviors. *Cell.* 2019;178(1):44-59 e47.
29. Vaanholt LM, Turek FW, Meerlo P. Beta-endorphin modulates the acute response to a social conflict in male mice but does not play a role in stress-induced changes in sleep. *Brain Res.* 2003;978(1-2):169-176.
30. Shair HN. Acquisition and expression of a socially mediated separation response. *Behav Brain Res.* 2007;182(2):180-192.

4. Discussion

In this thesis, we identified two factors contributing to the regulation of isolation-induced vocalization of mouse pups. First, we characterized USVs from mice with null expression of the paternal *Magel2* gene across the first 12 days of life. In summary, we found that at postnatal day 8, mutants vocalized less and had a limited vocal repertoire composed mostly of 'flat' and 'short' vocals, along with significantly less 'chevron' and 'step-up' vocals. Moreover, USVs were on average of lower duration and bandwidth. Second, in the following chapter, we characterized the effects of $POMC^{ARC}$ neurons and MOR on isolation-induced vocalization. We found that the activity of $POMC^{ARC}$ neurons reduces the emission of USVs and affects the composition of the vocal repertoire. Activation of $POMC^{ARC}$ neurons promotes the use of 'short' vocals and reduces the use of 'down-frequency modulation' and 'step-up' vocals. Here, I will discuss aspects of the emission of USVs and their spectral features as well as what these analyses can teach us about the mechanisms controlling the emission of isolation-induced vocalization.

4.1 Changes in Vocal repertoire and USV spectral features

The deficiency of *Magel2* and the activation of $POMC^{ARC}$ neurons reduced the emission of USVs and, at the same time, increased the use of 'short' and 'down-frequency modulation' vocals. These findings suggest that 'short' vocals could be a less salient signal than other more complex types of USVs. For example, 'down-frequency modulation' ranked first and 'short' ranked 2nd most used vocals for control pups in *Magel2* litters for ages P6-P10. At P12, pups use more of 'short' USVs than 'down-

frequency modulation' vocals. Mutant pups, on the other hand, use 'down-frequency modulation' the most at P6 but use 'short' the most from P8-P12. In another example, when we manipulated $POMC^{ARC}$ neurons, neuron activation leads to 'short' vocals being used most while neuron ablation leads to mostly 'down-frequency modulation' vocals instead. Together, these and other experiments suggest that the use of more of 'short' vocals is linked with lower use of isolation-induced vocalizations, which could be linked to a suppressed arousal state of the pups.

Overall, it is noticeable that the two most used vocalizations in the mouse strains tested did not differ with age or with the difference in isolation time. It is also interesting that manipulations of $POMC^{ARC}$ neurons did not modulate the spectral features of USVs, because another neuron population neighboring POMC neurons in ARC do. Agrp neurons, which are intermingled with POMC neurons in the ARC, can bidirectionally modulate the emission of USVs in mouse pups[1]. For example, impairing GABA transmission from these neurons results in a decrease in frequency, bandwidth, and duration of USVs[1]. However, modulation of $POMC^{ARC}$ neurons did not change any of these parameters related to the spectral features of the USVs. Therefore, there are potentially many mechanisms contributing to the production of USVs. Elucidating these different mechanisms can help understand how the internal state of the pups leads to the emission of different forms of USVs.

4.2 USV analysis from isolation-induced vocalizations

Our experiments manipulating isolation-induced vocalization behavior in pups have given us the opportunity to further understand what we can learn from vocal analysis. Here we analyzed spectral features including average, minimum, and maximum

frequency; we also analyzed bandwidth, duration, intensity, and harmonic components of USV emissions. As seen in Chapter 2, measurements of these features across all USVs were important in our understanding of changes in USV based on pup development.

Besides measuring vocal class emission, we also compared the distribution of probabilities that our vocal classifier gives for each USV. In other words, the machine learning algorithm that we used, while classifying each USV into one class, also gives the certainty (probability) that the given USV belongs to each of the classes. This distribution of probabilities is significant because it provides a more fluid classification of the vocalizations, likely better captures the biological nature of USVs compared to strict classifications. Using this distribution of probabilities—because there are 11 classes of USVs in our classifier, each USV has 11 probabilities and, therefore, 11 dimensions of data—we applied a dimensionality reduction algorithm to correlate USV structures between groups in Chapter 2. This analysis allowed us to capture a more in-depth view of the changes that occur in the vocal repertoire of mice and provide an example of analysis that can benefit the field as a whole, deepening our understanding of the vocal behavior in mice.

Given our findings, we also wish to highlight the importance of sampling infant vocalizations across different ages of preweaning mice. Our *Magel2* data found USV aspects different in some but not all tested ages from P6-P12. Moreover, preliminary data recording vocalization of pups at P15 and P18 under β-Endorphin knockout or Agrp neuron activation shows that vocal behavior ends closer to weaning age (P18) with some effects still apparent at P15. Additionally, peak vocal behavior age likely depends on strain genetics. Our preliminary work comparing infant USV profile of other

homozygous mouse strains found that peak age for vocal behavior expression varies by strain between P8, P10, or P12. Analyzing infant vocalization from its start to finish of this developmental period can help us understand how circuits manipulating this behavior change once pups transitions away from infant vocal behavior.

Moreover, we propose that all USV measurements should be analyzed across isolation time and development. While we did not do an extensive analysis of USV with temporal dynamics; it is likely that USV change throughout prolonged isolation. For example, in our POMC experiments, we found that time was a component influencing vocal rate during pup vocalizations when comparing time bins within each experimental group. In other words, during despair, pup vocal profile may change. Furthermore, it is possible to find effects not considered before by looking at prolonged isolation in pups. In our own preliminary studies of A/J mouse infant mice, we find that pups vocalize less during the first phase of isolation and increase vocal rate in the second half. This is contrary to the idea of protest preceding despair vocal behavior[2]. Hence, there is rich dataset that has been underutilized in the field of infant vocalizations that we hope will be brought into consideration in future studies.

4.3 Commentary on the role of infant vocalizations

Here I would like to posit that the goal of vocalizing is to find resources that maintain the body in optimal conditions; which are all provided by the caregiver. In other words, USVs serve as a means to forage for resources. USVs are already associated to gaining resources. For example, according to conflict theory, maternal genes balance energy expenditure between rear survival and her own while paternal genes selection mostly considers rear survival alone. Hence, paternal gene expression is focused on energy

intake and growth while maternal gene expression stunts growth and activity[3,4]. Moreover, in previous chapters we describe several examples of paternal imprint genes promoting USV emission and maternal imprint genes reducing USV emission; as well as examples of maternal neglect toward pups that vocalize less[5-7].

However, shifts between protest and despair phase in vocal behavior is likely an adaptive strategy to attract parental care during periods of social isolation. During long periods of isolation, pups undergo two different phases in vocal behavior: protest phase (high USV emission) and despair phase (low USV emission)[2,8]. We previously discussed despair behavior being a result of stress-induced analgesia. However, oscillation in vocal emission may have originally arise for unrelated reasons. For example, some animals engage in “Levy walk” while foraging[9,10]. The Levy walk is characterized by random bouts of activity (exploration) with time immobile in between (exploitation)[10]. Signs of this behavior exist from bacteria to mammals and it is thought to be an adaptive strategy to search for food in the wild[9,10].

As the field of infant vocalizations progress, it is important to understand the behavior’s function and the impact of deviation from standard USV in pup survival. In order to understand function, we must further explore how infant USVs affect maternal behavior through retrieval tests and play-back experiments. Additionally, we need to explore methods to accurately measure negative or positive emotional states in pups to better understand how to study and interpret data. Hence, I will conclude the thesis with a call of action: to hone tools and skills of systems neuroscience and behavior to explore ontogeny of innate behaviors as a way to approach a more holistic understanding of our own conduct and development.

4.4 References

1. Zimmer MR, Fonseca AHO, Iyilikci O, Pra RD, Dietrich MO. Functional Ontogeny of Hypothalamic Agrp Neurons in Neonatal Mouse Behaviors. *Cell.* 2019;178(1):44-59 e47.
2. Panksepp J, Watt D. Why does depression hurt? Ancestral primary-process separation-distress (PANIC/GRIEF) and diminished brain reward (SEEKING) processes in the genesis of depressive affect. *Psychiatry.* 2011;74(1):5-13.
3. Patten MM, Ross L, Curley JP, Queller DC, Bonduriansky R, Wolf JB. The evolution of genomic imprinting: theories, predictions and empirical tests. *Heredity (Edinb).* 2014;113(2):119-128.
4. Wilkins JF, Haig D. What good is genomic imprinting: the function of parent-specific gene expression. *Nat Rev Genet.* 2003;4(5):359-368.
5. Hernandez-Miranda LR, Ruffault PL, Bouvier JC, et al. Genetic identification of a hindbrain nucleus essential for innate vocalization. *Proc Natl Acad Sci U S A.* 2017;114(30):8095-8100.
6. McNamara GI, Creeth HDJ, Harrison DJ, et al. Loss of offspring Peg3 reduces neonatal ultrasonic vocalizations and increases maternal anxiety in wild-type mothers. *Hum Mol Genet.* 2018;27(3):440-450.
7. Nakatani J, Tamada K, Hatanaka F, et al. Abnormal behavior in a chromosome-engineered mouse model for human 15q11-13 duplication seen in autism. *Cell.* 2009;137(7):1235-1246.
8. Hennessy MB, Ritchey RL. Hormonal and behavioral attachment responses in infant guinea pigs. *Dev Psychobiol.* 1987;20(6):613-625.

9. Campeau W, Simons AM, Stevens B. The evolutionary maintenance of Levy flight foraging. *PLoS Comput Biol.* 2022;18(1):e1009490.

10. Cisek P. Resynthesizing behavior through phylogenetic refinement. *Atten Percept Psychophys.* 2019;81(7):2265-2287.